Deep Sea Research Part II: Topical Studies in Oceanography
June 2020, Volume 176, Pages 104774 (18p.)
https://doi.org/10.1016/j.dsr2.2020.104774
https://archimer.ifremer.fr/doc/00613/72461/

Connectivity between seamounts and coastal ecosystems in the Southwestern Indian Ocean

Crochelet Estelle [1, 2, *], Barrier Nicolas [3, 4], Andrello Marco [3, 4], Marsac Francis [3, 4], Spadone Aurélie [5], Lett Christophe [3, 4]

[1] ARBRE - Agence de Recherche pour la Biodiversité à la Réunion, 34 avenue de la Grande Ourse, 97434, Saint-Gilles, La Réunion, France
[2] IRD / ESPACE-DEV (UMR 228), Parc Technologique Universitaire, 2 rue Joseph Wetzell, CS 41 095, 97495, Sainte Clotilde Cedex, La Réunion, France
[3] Institut de Recherche pour le Développement (IRD), Sète, France
[4] MARBEC, Univ Montpellier, CNRS, Ifremer, IRD, Sète, France
[5] IUCN – International Union for Conservation of Nature, Gland, Switzerland

* Corresponding author : Etelle Crochelet, email address : estelle.crochelet@ird.fr

nicolas.barrier@ird.fr ; marco.andrello@gmail.com ; francis.marsac@ird.fr ; aurelie.spadone@iucn.org ; christophe.lett@ird.fr

Abstract :

Understanding larval connectivity patterns is critical for marine spatial planning, particularly for designing marine protected areas and managing fisheries. Patterns of larval dispersal and connectivity can be inferred from numerical transport models at large spatial and temporal scales. We assess model-based connectivity patterns between seamounts of the Southwestern Indian Ocean (SWIO) and the coastal ecosystems of Mauritius, La Réunion, Madagascar, Mozambique and South Africa, with emphasis on three shallow seamounts (La Pérouse [LP], MAD-Ridge [MR] and Walters Shoal [WS]). Using drifter trajectory and a Lagrangian model of ichthyoplankton dispersal, we show that larvae can undertake very long dispersion, with larval distances increasing with pelagic larval duration (PLD). There are three groups of greater connectivity: the region between the eastern coast of Madagascar, Mauritius and La Réunion islands; the seamounts of the South West Indian Ridge; and the pair formed by WS and a nearby un-named seamount. Connectivity between these three groups is evident only for the longest PLD examined (360 d). Connectivity from seamounts to coastal ecosystems is weak, with a maximum of 2% of larvae originating from seamounts reaching coastal ecosystems. Local retention at the three focal seamounts (LP, MR and WS) peaks at about 11% for the shortest PLD considered (15 d) at the most retentive seamount (WS) and decreases sharply with increasing PLD. Information on PLD and age of larvae collected at MR and LP are used to assess their putative origin. These larvae are likely self-recruits but it is also plausible that they immigrate from nearby coastal sites, i.e. the southern coast of Madagascar for MR and the islands of La Réunion and Mauritius for LP.

Keywords : Seamounts, connectivity, larval duration, larval drift, Lagrangian modelling, biophysical model, surface drifters, Southwestern Indian Ocean, Ichthyop.

1. Introduction

Marine resources are under threat from the combined effects of climate change, overfishing, pollution, diseases, tourism and coastal development (FAO, 2018). As marine ecosystems degrade, so do the well-being and livelihoods of populations that depend directly on the ecosystem goods and services they provide (Moberg and Folke, 1999). Managing marine resources effectively is therefore crucial, from both social and ecological perspectives. Connectivity is recognized as a key factor affecting marine populations dynamics, population persistence and stock sustainability (Hastings and Botsford, 2006), as well as the efficiency of management strategies in the face of global changes. It is defined as "the exchange of individuals among geographically separated subpopulations" (Cowen et al., 2007). Transport processes are believed to connect distant populations. Despite early genetic studies showing a fair degree of homogeneity between populations over large spatial scales (Doherty et al., 1995), accumulating recent evidence suggests that populations are not as open as initially thought. High levels of local retention and low levels of long-distance dispersal could be maintained by mesoscale and sub-mesoscale eddies capable of transporting larvae back to their location of origin despite long pelagic larval durations (Cowen et al., 2000; Warner and Cowen, 2002), thereby contributing to maintain endemic species around isolated islands (Boehlert et al., 1992).

The majority of marine organisms have a bipartite life history and experience pelagic larval stages before they settle and become sedentary (Leis, 1991). Larvae remain in the midwater layers for days to months while they acquire swimming and sensory capabilities that enable them to control part of their dispersal (Kingsford *et al.*, 2002; Leis, 2002). This pelagic stage facilitates the transport of individuals among spatially isolated populations. It has been suggested that the pelagic larval duration (PLD) is the most important factor determining the

level of larval dispersal and connectivity (Riginos and Victor, 2001; Selkoe and Toonen, 2011; Luiz et al., 2013). Connectivity between distant populations may indeed be favoured by long PLD, whereas larval settlement close to the natal habitat can result from short PLD and entail increased population differentiation over short scales (Planes et al., 2001). However, larval dispersal is also mediated by both complex and dynamic oceanographic features and biological properties (Pineda et al., 2009).

The effective management of marine resources requires estimating the realized levels of connectivity between populations, but empirical estimates are scarce (Manel et al., 2019). Indeed, marine larvae are notoriously difficult to monitor, due to their small size and possibly long dispersal distances, up to hundreds of kilometers from their initial release site (Leis, 1984; Victor, 1987). Patterns of larval dispersal and connectivity also vary between species. Various methods such as population genetics and phylogeography, microchemical fingerprinting, stable isotopes, otolith microchemistry, otolith shape analysis and biophysical dispersal models have been developed to assess patterns of larvae dispersal and population connectivity across the marine environment (Schultz and Cowen, 1994; Roberts, 1997; Cowen et al., 2000; Hellberg, 2007; Treml et al., 2008; Jones et al., 2009; Mora et al., 2012, Bryan-Brown et al., 2018).

The South West Indian Ocean (SWIO) has a high level of marine biodiversity, and marine species in the region are widely used as food resources and provide economic benefits to a rapidly growing human population. However, the SWIO is one of the less studied regions of the world (Obura, 2012; UNEP-Nairobi Convention and WIOMSA, 2015).

The SWIO has many seamounts. Seamount ecosystems are recognized as critical habitats for a wide array of species (Clark et al., 2012) and are subject to anthropogenic exploitation (Rowden et al., 2010). Despite an increased focus on these particular ecosystems, the natural processes involved to sustain biodiversity at seamounts remain largely unknown, in particular in the SWIO. Seamounts are generally geographically isolated structures, but currents can ensure connectivity between them and with adjacent ecosystems.

In this paper, we consider nine seamounts of the SWIO, ranging from latitudes 15°S to 45°S (Figure 1), which were the focus of previous oceanographic campaigns (Southern Indian Ocean Seamounts Project in 2009: Read and Pollard, 2017; Rogers et al., 2017; Pollard and Read, 2017). Five of them belong to the South West Indian Ridge (SWIR, 25–50°S), an area delineated by elevated rims reaching up to 2000 m below sea level, with several seamounts on its flanks rising to only a few hundred metres below the surface (Guinotte, 2011): Atlantis Bank, Sapmer Bank, Middle of What Seamount, Melville Bank and Coral Seamount. The SWIR is crossed by subtropical and Agulhas Return Current convergences (Figure 1). These strong hydrological discontinuities are almost impassable by small size organisms, both in the adult and larval stages. There is therefore no genetic connectivity between populations north and south of the subtropical convergence line (Rogers, 2012). We include three other seamounts located on the Madagascar Ridge: two unnamed pinnacles – hereafter called MAD-Ridge and Un-named seamount respectively) and Walters Shoal. The rugged topography and numerous shoals on this portion of the Madagascar Ridge interact with ocean currents (Roberts et al., 2020, this issue; Vianello et al., 2020, this issue). MAD-Ridge is a steep pinnacle (33 km north–south; 22 km east–west) located 240 km south of Madagascar and rises to 240 m below the surface. It is under the influence of a highly dynamic ocean circulation (the East Madagascar Current and its retroflection, Figure 1; de Ruijter et al.,

2004) inducing strong mesoscale activity (Pollard and Read, 2017; Vianello et al., 2020, this issue). Indeed, it is frequently crossed by mesoscale eddies spinning off the South East Madagascar Current. These eddies may become trapped over the seamount and have an influence on the assemblages and diel vertical migrations patterns of micronekton communities (Annasawmy et al., 2020, this issue). Walters Shoal and Un-named seamount are very isolated features (>800 km south of Madagascar, 1300 km off the South African coastline) located at the southern end of the Madagascar Ridge. Both seamounts are classified as Benthic Protected Areas by the Southern Indian Ocean Fisheries Agreement (Shotton, 2006; SIOFA, 2019). Walters Shoal is a large seamount rising to 18 m below the surface located 855 km south of Madagascar. Previous investigation showed a 400 km^2 caldera-like shape of the summit (RV Marion Dufresne cruises in 1973 and 1976, unpublished data). It has moderate mesoscale dynamics (Pollard and Read, 2017). The last seamount considered, La Pérouse, is located 160 km northwest of La Réunion Island. It is under the influence of the west-flowing South Equatorial Current (SEC, Figure 1) (Tomczak and Godfrey, 2003; Chapman et al., 2003) and has moderate mesoscale dynamics. As an old volcano, La Pérouse rises steeply to 55-60 m depth from the abyssal plain at 5000 m and is 10 km long (Marsac et al., 2020, this issue).

We also considered eight coastal sites, where knowledge on species and/or circulation were available, to assess exchanges with the seamounts: (i) two Mascarene archipelago sites, the west coast of Mauritius (Morne Brabant) and La Réunion (La Saline); (ii) four sites in Madagascar (Sainte-Marie and Mamanjary on the east coast, Fort-Dauphin in the south and Tulear in the southwest); and (iii) two sites on the African coast (Tofo in Mozambique and Saint Lucia in South Africa) (Figure 1). As these coastal sites are not fully representative of the respective coastlines, we also defined buffers around countries (Mauritius, La Réunion,

Madagascar, Mozambique and South Africa), 1/3° from shore, to highlight larval export from seamounts to surrounding countries.

The aim of this paper is to assess the degree of connectivity, deduced from hydrodynamic larvae dispersion, between the nine selected SWIO seamounts and nearby coastal ecosystems represented by the eight coastal sites and also nearby countries. Emphasis is placed on the three shallow seamounts which are the focus of the present Special Issue: La Pérouse (LP – doi:10.17600/16004500), MAD-Ridge (MR – doi:10.17600/16004900) and Walters Shoal (WS – doi:10.17600/17002700) (Roberts et al., 2020, this issue). In order to characterize connectivity patterns, we first used drifter trajectory data as evidence for possible hydrodynamic connectivity. Then, to gain a broader view of connectivity patterns, we used Ichthyop, a Lagrangian model (Lett et al., 2008) to simulate ichthyoplankton dispersal. This model was forced by near-surface ocean current estimates (OSCAR). A wide range of PLD values were considered to provide a synoptic view of seamount connectivity. Finally, we used information on PLD and the age of larvae collected at MR and LP by Harris et al. (2020, this issue) to assess their putative origin.

2. Material and methods

2.1 SWIO marine species

More than 800 fish species have been recorded on seamounts worldwide (Morato et al., 2004). Most are robust demersal fish species, with good swimming capabilities, high food consumption and energy expenditure. Some of them also exhibit great longevity (over 100 years) with late maturation (50-60 years) and low fertility, making them extremely vulnerable to intensive fishing (Koslow et al., 2000).

Soviet and Ukrainian fisheries operating from 1969 to 1998 in the SWIO identified 81 fish families including four *Beryx* species (alfonsinos, including *Beryx splendens* and *B. decadactylus*) and orange roughy (*Hoplostethus atlanticus*) of high commercial value, pelagic pentacerotidae (*Pseudopentaceros wheeleri*, *P. richardsoni*), rockfish (*Sebastes* spp., *Helicolenus* spp.), oreos (Oreosomatidae), cardinal fish (*Epigonus* spp.), grenadiers (including *Coryphaenoides rupestris*) and Patagonian toothfish (*Dissostichus eleginoides*) (Romanov, 2003). These fish are specifically associated with seamounts, although they also live on the continental slopes and slopes of oceanic islands. Soviet and Ukrainian fisheries also inventoried a minimum of 13 threatened species of shark (Romanov, 2003) and benthic resources such as crustaceans (lobsters, crabs), molluscs, sponges, and cold-water corals. A new species of spiny lobster, *Palinurus barbarae* (Groeneveld et al., 2006), appears to be endemic to the Walters Shoal (WS), as well as the crab *Beuroisia duhameli* (Guinot and Richer de Forges, 1981) caught during the MD08 campaign of RV Marion-Dufresne in 1976. More recently, cruises to La Pérouse (LP), MAD-Ridge (MR) and the WS seamounts allowed identification of several micronekton species. Annasawmy et al. (2019) reported vertically migrating common open-water species of gelatinous crustaceans, squid and fish concentrated over the summit and flanks, and also an important community of seamount-associated/resident fish. Harris et al. (2020, this issue) also collected mesopelagic fish larvae during the current cruises, Myctophidae and Gonostomatidae being the most dominant families at all three seamounts.

Despite these valuable recent data, biological data on marine species inhabiting SWIO seamounts are generally lacking, as underlined in several publications (Rogers, 2012; FFEM, 2013; Rogers et al., 2017; Zucchi et al., 2018). In particular, there is only limited information available on their PLD for ichthyological species recorded during sea campaigns (e.g.

Pseudopentaceros richardsoni, *Hoplostethus atlanticus*, *Beryx splendens*), which have PLDs ranging from one to several months. Hence, *Beryx* spp. may have a PLD of around one year (Shotton, 2016). *Jasus* spp. (spiny lobsters) were recorded in seamount habitats in the southern hemisphere and are also known to have long PLDs. Hence, Booth (2006) reported PLDs between 8 and 12 months for *J. verreauxi*, and between 12 and 24 months for *J. edwardsii*. Harris et al. (2020, this issue) provided information on specimens collected at MR of the acanthurid *Naso* sp. having a PLD of 84 d, *Labrid* spp. with a PLD of 26–28 d, *Apogon* spp. with a PLD of 18–34 d and *Synodus sp.* with a PLD of 42 d (Stier et al., 2014). Thus, the different species inhabiting the SWIO seamounts cover a large range of PLD values.

2.2 Oceanographic drifter trajectories

As a first approach to assessing dispersal and connectivity in the SWIO, we downloaded 6-h interpolated trajectories of 1104 drogued oceanographic surface drifters located in the SWIO over the period 15/02/1979 to 30/06/2018 from the Global Drifter Program database (https://data.nodc.noaa.gov/cgi-bin/iso?id=gov.noaa.nodc:AOML-GDP, Lumpkin and Centurioni, 2019). From that dataset, we selected drifters that came close (<50 or 100 km) to one of the three focus seamounts (LP, MR and WS) and plotted their trajectories. We also searched for drifters that came close to two of the same seamounts, as an indication of possible hydrodynamic connectivity between seamounts.

2.3 Ichthyop larval dispersal model

To gain a broader perspective of dispersal and connectivity in the SWIO, we used the larval dispersal tool Ichthyop, a free Lagrangian tool designed to study the effects of physical and biological factors on ichthyoplankton dynamics (Lett et al., 2008). Ichthyop can integrate the most important processes involved in the early life stages of marine larvae: spawning,

transport, behaviour, growth, mortality and settlement. As we wished to obtain a synoptic view of connectivity patterns, rather than focus on a particular species, we used a large range of PLD values (15, 30, 45, 60, 90, 120, 180, 270 and 360 d) and assumed that all seamounts had habitats and populations capable of both producing and receiving larvae. This latter assumption is supported by the findings of Harris et al. (2020, this issue) who reported all developmental stages of oceanic and some neritic taxa from preflexion to postflexion at LP, MR and WS, an indication that the corresponding species spawn in the vicinity of these seamounts. We also assumed that larvae were transported passively depending only on horizontal surface currents. The term “larvae” used in the modelling part of this paper really stands for “virtual larvae” because there were no ground truth data to calibrate and validate the model. Particles were released every 5 d over 9 years, i.e. 10 000 particles at each of the considered release locations, a number that was shown to be large enough to provide precise estimates of connectivity values (Andrello et al., 2013). Release locations (Figure 1) were the nine SWIO seamounts and the eight coastal sites described in the introduction. Potential larval destination areas were the nine SWIO seamounts, the eight coastal sites and the shorelines of the five countries (Mauritius, La Réunion, Madagascar, Mozambique and South Africa; Figure 1). Simulations were performed with two sizes of buffer around locations used as release and destination areas, 1/3 of a degree and 1 degree.

As expected, the simulated values of connectivity were overall greater with a 1° buffer than with a 1/3° buffer, but as the connectivity patterns (i.e. sites that are more/less retentive, more/less connected, etc.) were similar, we only present the 1/3° case and refer the reader to Appendix Figure E for the 1° buffer results. The Ichthyop model was forced by current fields provided by the OSCAR product (see below) interpolated linearly at the location and time of

each larva, and their movement was solved using the Runge Kutta 4th order scheme, diffusion being added with a dissipation rate ε=1 E^{-9} m^2 s^{-3} (following Peliz et al., 2007).

2.4 OSCAR current product

OSCAR (Ocean Surface Current Analyses – Real Time) provides estimates of ocean near-surface currents by combining satellite-derived altimetry observations (sea-surface height; e.g. TOPEX/Poseidon), scatterometer data that estimate ocean wind vectors, and sea surface temperature sensors (e.g. AVHRR). OSCAR provides more precise ocean current estimates than those based exclusively on altimetry, particularly in the tropics, by combining geostrophic shear dynamics, Ekman and Stommel transport and a complementary term of surface buoyancy gradient (Bonjean and Lagerloef, 2002). Products are available worldwide at 1/3° horizontal resolution every 5 d and represent currents at a depth of ~15 m. Here we used the currents data for the SWIO (latitude 10–50°S, longitude 20–70°E) over the period 2010–2018, downloaded from the NASA data center website (ftp://podaac-ftp.jpl.nasa.gov/allData/oscar/preview/L4/oscar_third_deg/). OSCAR products were validated for the northern part of the Indian Ocean by Sikhakolli et al. (2013).

2.5 Model outputs and post-processing

We calculated connectivity matrices between seamounts, between seamounts and coastal ecosystems, and between coastal ecosystems and seamounts for all the considered PLD values averaged over all release dates. Connectivity can be interpreted as either the proportion of larvae exported to each seamount or coastal ecosystem (larval export, lines of the connectivity matrices), or the proportion of larvae coming from each seamount or coastal ecosystem (larval import, columns of the connectivity matrices). Local retention, i.e. the proportion of released larvae that stayed at their natal sites, is the diagonal of the connectivity matrices. We also

computed the dispersal distance as the "great-circle distance" between the initial and final positions of larvae, averaged for all larvae and release dates. We plotted maps of simulated larval density, the average number of all larvae per cell at a given time. The cell size was set as 1/3°, equivalent to the OSCAR resolution. Analyses were carried out using the software ArGIS 10.4.1 and Spyder (Python 2.7).

3. Results

3.1 Drifters

We found 13, 11, and 14 drifters passing less than <50 km from the LP, MR and WS seamounts, respectively, at some time in their travel in the SWIO (Figure 2). Most (11/13) drifters that came close to LP ended up to the south in the direction of the other seamounts (Figure 2a). One drifter (#45958) that came very close to LP (~ 7 km) was also close to MR (~ 8 km) 85 d later (the trajectory of that drifter is highlighted by a white background in Figure 2a). Drifters that travelled close to MR moved to the west or to the east and none travelled to LP or WS (Figure 2b). Most (10/14) drifters that came close to WS ended up to the west (Figure 2c), but along the way one drifter (#63941330) came close (~ 43 km) to MR after 75 d (the trajectory of that drifter is highlighted by a white background in Figure 2c).

We found 32, 23 and 21 drifters that travelled <100 km from LP, MR and WS, respectively (Appendix Figure A). Among those, six drifters came close to LP and then MR (with 46–189 d spent in between), two drifters travelled close to MR and then WS (29 and 70 d spent in between) and two drifters came close to WS and then MR (75 and 143 d spent in between). One of those drifters (#9108691) is of particular interest because it came close to first LP (~51 km), then MR (~71 km) and finally WS (~18 km), and was the fastest drifter, travelling from

LP to MR in 46 d and from MR to WS in 29 d (the trajectory of that drifter is highlighted by a white background in Appendix Figure A).

3.2 Mean dispersal distances

In the simulations, as expected, the mean dispersal distances travelled by the virtual larvae leaving seamounts increased with PLD, ranging from 217 km for PLD = 15 d to 1366 km for PLD = 360 d, all seamounts averaged (Table 1). Larvae leaving Atlantis Bank had the shortest average dispersal distances (around 0.6 times less than the mean) except for PLD = 15, where the shortest distance was for larvae leaving WS (Table 1). Conversely, larvae from Coral Seamount had the highest mean dispersal distances for all PLD (1.5–2.15 times above the mean). For the three focal seamounts, larvae released from WS travelled the shortest average distances, whereas larvae leaving MR travelled farthest.

3.3 Connectivity matrices between all sites

Matrices presented in Figure 3 show the mean simulated larval connectivity obtained between all nine seamounts and eight coastal sites for three of the considered PLD values: 15, 120 and 360 d (matrices for the six other PLD values are provided in Appendix Figure B). For a PLD of 15 d (Figure 3a), there were bilateral exchanges between Morne Brabant (Mauritius coastal site), La Saline (La Réunion coastal site) and LP, one of our three focal seamounts. For the other two seamounts, there was also bilateral exchange between WS and Un-named Seamount (which are close) and between MR and Fort Dauphin. The highest local retention values were for WS (11.1%), Atlantis Bank (7.5%) and LP (5.3%), in decreasing order. For a PLD of 120 d (Figure 3b), there was bilateral connectivity between the five sites situated East of Madagascar (Maurice, La Réunion, LP, Mamanjary, Ile Ste Marie) and most of the seven sites located south of Madagascar and in the Mozambique Channel (WS, Un-named Seamount,

MR, Fort Dauphin, Tulear, Tofo, Saint Lucia). Finally, there was connectivity between most of the five seamounts situated on the SWIR (Atlantis Bank, Sapmer Bank, Middle of What Seamount, Melville Bank, Coral Seamount), attaining an elevated degree between Sapmer Bank, Middle of What seamount and Melville Bank. There was also bilateral exchange between WS and MR, LP and MR, and WS and LP. For a PLD of 360 d (Figure 3c), most sites were connected in both directions to some extent: the SWIR and South Madagascar seamounts group tended to join. WS, MR and LP were connected bilaterally to all seamounts and coastal sites, with the sole exception of LP which did not receive any larva from Saint Lucia. We assessed the temporal variability (seasonal and interannual combined) of simulated connectivity for the different PLD values (Appendix Figure C) and obtained little variability with coefficients of variation (CV) of 2.7 at most. The CV tended to decrease with PLD, and to have similar values for seamounts within the three different identified groups, i.e. east Madagascar, south Madagascar and Mozambique Channel, and SWIR, and also between two different groups (hence the “blocks” of similar colours in Appendix Figure Cc).

3.4 Connectivity matrices between LP, MR and WS seamounts and coastal ecosystems

Figure 4 represents exchanges from seamounts to coastal ecosystems (coastal buffers) for PLD values of 15, 120 and 360 d (matrices for the six other PLD values are in Appendix Figure D).

After 15 d of dispersal, connectivity ranged from 0 to 2.1%. Larvae released at LP reached the coastal ecosystems of Mauritius (0.007%), Madagascar (0.03%) and La Réunion (2.1%), whereas larvae from MR only reached Madagascar. After 120 d, larval connectivity values were divided by ~5, ranging between 0 and 0.42%. Larvae from LP reached all coastal ecosystems (Mauritius, La Réunion, Madagascar, Mozambique and South Africa). The two highest connectivity values were between LP and Madagascar (0.42%) and between LP and

La Réunion (0.21%). Larvae from MR also reached all coastal ecosystems, but with lower connectivity values. Larvae from WS reached all coastal ecosystems except Mauritius, with even lower connectivity values. After 360 d of dispersal, larval connectivity values were divided by ~10 relative to PLD = 120 d. All larvae leaving LP, MR and WS reached all coastal ecosystems. Overall, the lowest connectivity was from WS, except to Mozambique where it was the highest.

3.5 Larval dispersal from LP, MR and WS

The patterns of weak connectivity between seamounts and the coast described above result from a high degree of dispersal towards offshore locations, as shown by maps of larval density over the entire region. Figure 5 presents mean larval density maps for larvae released at LP, MR and WS seamounts after 15, 120 and 360 d of PLD (with the locations of the drifters of Figure 2 superimposed). Larvae released from LP remained concentrated at high density on the eastern side of Madagascar for a PLD of up to 120 d, and then tended to drift east. After 120 d, larvae released at MR split into two separate plumes, one directed east and the other west towards the South African coast. Larvae released at WS remained concentrated around that seamount for a longer time, eventually spreading east and west, similarly to larvae released at MR.

3.6 Local retention and connectivity between LP, MR, and WS

Local retention decreased with increasing PLD for all three seamounts, but at a faster rate for LP than for MR and WS (Figure 6). Conversely, connectivity between pairs of seamounts initially increased with increasing PLD values (Figure 7). Patterns of connectivity change with PLD and were similar for MR to WS, MR to LP, and WS to MR, first increasing strongly, then peaking around 120 d and eventually decreasing slightly for longer PLDs.

Connectivity between the most distant sites, WS and LP, was much weaker and continued to increase with PLD in the range of values tested. Connectivity from LP to MR was at an intermediate level and showed the least change with PLD.

3.7 Larval import at LP, MR and WS

The origin of larvae reaching LP, MR and WS is shown in Figure 8 after PLDs of 15, 120, and 360 d. At 15 d, larvae reaching WS, MR and LP were mostly self-recruits (95%, 95% and 77%, respectively). For a PLD of 120 d, there was still a lot of self-recruitment at WS (42%) and MR (38%), but not at LP (15%), at which 57% of larvae came from Madagascar. At 360 d, there was still 27% of self-recruitment on WS and no larvae coming from LP. The pattern was similar for MR, but with only 17% of self-recruitment. For LP, there was only 9% of self-recruitment, with the balance of larvae originating from MR (15%), WS (2%), Mauritius and La Réunion (20%), Madagascar (37%) and other seamounts (10%).

3.8 Link with ichthyoplankton data

It is difficult to interpret the above results in a biological sense because the larval durations of the species inhabiting the seamounts are poorly known. However, Harris et al. (2020, this issue) provide useful information on PLD and age for a set of larvae they collected at MR and LP. In particular, at MR, they collected larvae of four species with estimated PLDs close to 30 d (*Labrid* and *Apogon* spp.), 45 d (*Synodus* sp.) and 90 d (the acanthurid *Naso* sp.). Assuming that these species reproduce at all the sites under consideration, dispersal patterns can be obtained for these PLD values (Figure 9) and also larval import and export for MR, where most larvae were collected (Figure 10). For a PLD of 30 d, virtual larvae arriving at MR originated from Fort Dauphin, MR and Un-named seamount (Figure 10). For a PLD of 45 d,

virtual larvae arriving at MR originated from Saint Lucia, Tofo, Fort Dauphin, MR, Unnamed seamount and WS. For a PLD of 90 d, they originated from all 17 release sites.

Harris et al. (2020, this issue) also provide age estimates for some of the larvae they collected. All larvae collected at MR were in the range 1.4-16.2 d, a range is largely consistent with the ages of virtual larvae transported from Fort Dauphin to MR in our simulations (Figure 11a). Ages of virtual larvae transported from Mamanjary to MR (>10 d, Figure 11b) suggest that the oldest larvae collected, such as *Synodus* and *Trachinocephalus myops*, may also have been transported from there. At LP, all larvae collected except one (a macrourid species) have estimated ages >5 d and may therefore have been transported from La Saline (Figure 11c), whereas collected larvae >10 d (*Vinciguerria* spp.) may also have come from Morne Brabant (Figure 11d). Of course, all larvae collected could also have been self-recruits.

4. Discussion and perspectives

The aim of this work was to assess the degree of connectivity between nine seamounts of the South West Indian Ocean (SWIO) and nearby coastal ecosystems, with emphasis on three shallow seamounts: La Pérouse (LP), MAD-Ridge (MR) and Walters Shoal (WS). The Lagrangian model of larval dispersal allowed us to explore a wide range of pelagic larval durations (PLDs) and revealed robust patterns of larval connectivity.

4.1 Mean drift velocities and larval dispersal distance

Larvae dispersed far from their site of origin, with travelled distances increasing with PLD. Mean drift velocities, obtained by dividing the mean larval distances reported in Table 1 by PLD, reached values as high as 10 km d^{-1} (about 0.1 m s^{-1}). Such values are consistent with current surface velocities found by Pollard and Read (2017) and Vianello et al. (2020, this

issue) during the MAD-Ridge cruise. They are also of the same order of magnitude as other estimates obtained by Lagrangian simulations in other regions. For example, median drift velocities were about 4 km d^{-1} in the Mediterranean Sea (Andrello et al., 2013). Other connectivity studies performed in the SWIO have highlighted long-distance colonization, possibly over several generations, between coral reefs (Crochelet et al., 2016), between South African ecosystems and La Réunion for vagrant dusky groupers (Reid et al., 2016), between Mauritius and La Réunion for honeycomb groupers (Crochelet et al., 2013), between the Mascarene archipelago and Madagascar for tropical eel (Pous et al., 2010) and Seychelles for Sargassum algae (Mattio et al., 2013), between the east African coast and Madagascar for mangrove propagules (Van der Stocken and Menemenlis, 2017) and for coral reef species (Gamoyo et al., 2019; Schleyer et al., 2019), and between ABNJ (Areas Beyond National Jurisdiction) and coastal zones (Popova et al., 2019, Maina et al., 2020). Our results focusing on seamounts show that currents around SWIO seamounts can be powerful means of larval dispersal over relatively long distances. The longest dispersal distances were obtained from the Coral Seamount, the southernmost seamount considered in this study, which is affected by the strong current velocities of the Agulhas Return Current.

4.2 Potential colonization of coastal sites by larvae originating from seamounts

Connectivity from seamounts to coastal ecosystems was weak, with a maximum of 2.1% larvae originating from seamounts reaching coastal ecosystems. It is difficult to conclude whether such a low percentage of dispersal is good enough to influence the communities of the receiving sites, because the magnitude of immigration depends on survival during the pelagic phase and on local dynamics (Armsworth, 2002; Burgess et al., 2014). If a population is not self-sustaining as a consequence of high mortality or low fecundity rates, then immigration from other populations contributes to population persistence. Although some of

the seamounts mentioned herein are subject to fishing (with strong impacts on stocks of long-living species), coastal ecosystems are affected by greater anthropogenic pressure (e.g. fishing, dredging, pollution) and generally have smaller biomasses than isolated sites (Edgar et al., 2014; Cinner et al., 2016). Therefore, seamounts could be important sources of larvae for coastal sites, if connectivity is strong enough to transport sufficiently high numbers of larvae over long oceanic distances and the receiving habitat is appropriate. Owing to the lack of data on local population dynamics and abundance in both the seamounts of origin and the coastal sites of destination, however, this hypothesis cannot be tested here.

4.3 Local retention at seamounts and connectivity between seamounts

Local retention (within a 1/3° buffer) at the three focal seamounts (LP, MR and WS) was also low, peaking at about 11.1% at the shortest PLD and decreasing sharply at longer PLDs. These values may be an underestimation of actual patterns of local retention, however, because of the relatively coarse spatial resolution of the ocean current product (OSCAR) and, perhaps more importantly, the assumption of passive larval dispersal, because active swimming and larval orientation mechanisms can increase local retention (Faillettaz et al., 2018). Even if retention probabilities seem low, though, they might be sufficiently high to replenish populations and ensure their persistence because of high fecundities of the fish species. For example, large female alfonsino (*Beryx splendens*) spawn a range of 0.8–2.4 million eggs (Alekseeva, 1983). We also found that local retention was greater at WS than at MR (Figure 6), which is consistent with Vianello et al. (2020, this issue) showing that currents decrease from north to south along a transect going from MR to WS.

Maina et al. (2020) recently used a modelling approach similar to the one used here to assess connectivity between seamounts of the SWIO using a PLD of 30 d. Here, we used a range of

PLD values from 15 to 360 d and showed that connectivity patterns change dramatically with PLD. Here we obtained large differences in dispersal and connectivity patterns for PLD values of 30, 45 and 90 d, which correspond broadly to labrid and *Apogon* spp., *Synodus* sp., and acanthurid *Naso* sp., respectively, collected by Harris et al. (2020, this issue) at MR (Figure 10). Therefore, differences in the putative origin of these collected larvae were significant (Figure 9), although a local (i.e. MR) origin was the most likely for all of them. For some species, the presence of larvae, juveniles and adults around the same seamount suggests that their populations are self-sustaining (Cherel et al., 2020, this issue). For neritic reef-associated species, it is also plausible that some of the larvae collected at MR originated from the south-east coast of Madagascar (Harris et al., 2020, this issue). Indeed, MR has a strong connection with the shelf waters through cross-shelf transport. This suggestion is supported by our age analysis of larvae, which shows that larvae arriving at MR may come from Fort Dauphin or Mamanjary (Figure 11). Similarly, it is also possible that larvae collected at LP come from the islands of La Réunion and Mauritius (Figure 11).

Connectivity patterns between seamounts revealed three groups of greater connectivity: the region between the eastern coast of Madagascar, Mauritius and La Réunion islands; the seamounts of the SWIR; and the pair Walters Shoal – Un-named seamount. Connectivity between these three groups was only at long PLDs.

With the exception of the two lowest connectivity values (between WS and LP), connectivity peaked at around 120 d PLD and remained stable or slightly decreased at longer PLDs (Figure 7). However, that pattern does not consider the effects of larval mortality, which are likely to reduce connectivity proportionally to PLD.

We found little temporal variability in simulated connectivity patterns, which is consistent with Vianello et al. (2020, this issue) who reported no clear seasonality or interannual variability in currents along the Madagascar Ridge.

4.4 Complementarity of drifter data and Lagrangian simulations

Drifter data were used as ground-truth information of hydrodynamic dispersal and connectivity, and they consolidated the results of Lagrangian modelling. Indeed, the trajectories followed by drifters passing close to each of the three focal seamounts were consistent with the general patterns followed by particles released there. In addition, we found drifters passing LP and then MR, passing WS and then MR, and passing LP and then MR and WS, which were also among the strongest connections found between seamounts in the Lagrangian model (Figure 7). Besides this, the range of time spent by drifters travelling from LP to MR (46–189 d) corresponded well with the PLD values for connectivity between these seamounts in the model. The range of time spent by drifters between the other seamounts (29–70 d from MR to WS, 75–143 d from WS to MR) were also consistent with the model results, although slightly slower. However, we found no drifter passing MR and then LP, although that is one of the strongest connections according to simulation results (Figure 7).

4.5 Limitations of the modelling approach

Numerical transport models are increasingly being used to determine patterns of larval dispersal as well as connectivity between populations in the marine environment. Larval dispersal simulations are relatively simple and quick to implement in any study region. Indeed, data necessary for model input (coastline, release sites, etc.) are freely available online at high resolutions. Nevertheless, the work accomplished during this study could be improved by taking into account additional oceanographic and biological factors.

We used an ocean current product (OSCAR) that relies on remote-sensing data to force the Lagrangian larval dispersal model. OSCAR currents are available globally and over long periods of time. Despite their coarse spatial resolution (1/3°), OSCAR and other products providing near-surface ocean current estimates have been shown to allow the simulation of surface drifter trajectories with similar accuracies as outputs from oceanographic models of similar spatial resolution (Liu et al., 2014; Amemou et al., submitted).

However, OSCAR does not take into account the vertical stratification of currents in the water column, which may affect larval dispersal patterns. In this study, larvae were considered as passive particles drifting in the surface layer, because we had no knowledge of the larval biology of local species. However, the larvae of many species have good swimming ability (Fisher et al., 2005) and are capable of changing their behaviour (e.g. by changing their depth) in response to the environment (Leis and Carson-Ewart, 2002; Tolimieri et al., 2000). This affects how larvae are carried by currents (Irisson et al., 2010; Cherubin et al., 2011), because transport is usually faster close to the surface than in the deeper layers. Larvae might therefore rely on vertical migration to reduce their dispersal and promote local retention (Cowen, 2002). When such information is available, it is therefore important to consider larval behaviour and swimming capability during larval ontogeny (Leis, 2010), and physical data such as vertical stratification of currents.

Vianello et al. (2020, this issue) reported no clear seasonality or interannual variability in currents along the Madagascar Ridge. Nevertheless, Annasawmy et al. (2019) highlighted a strong seasonality in primary productivity at LP and MR, with maximum values reached in July, as a result of intense mixing caused by the austral winter trade winds, and minimum

values during the austral summer (December–March). Moreover, chlorophyll a (Chl-a) concentrations were twice as high at MR than at LP all year round. This seasonality and the differences between seamounts may have consequences on secondary productivity and thus on food availability, growth and survival for larvae. Harris et al. (2020, this issue) also showed that different environmental variables such as temperature, Mixed Layer Depth (MLD), Depth of Chlorophyll Maximum (DCM), zooplankton settled volume and integrated Chl-a, influence larval fish communities at LP, MR and WS. Therefore, environmental factors and their effect on biological processes such as larval growth and mortality are important factors to consider in future modelling studies.

4.6 Perspectives

From the perspective of the conservation and management of ecosystems, in particular in areas beyond national jurisdiction (ABNJ) where most SWIO seamounts are located, improving the understanding and knowledge of larval dispersal is crucial. A new, legally binding instrument for the high seas has been discussed since 2006 under the United Nations Convention on the Law of the Sea for the conservation and sustainable use of marine resources beyond national jurisdiction. Larval dispersal will be a key point in designing regional networks of Marine Protected Areas (Andrello et al., 2017) to conserve biodiversity in the high seas efficiently. Studies using numerical models in combination with the data and knowledge gathered during at-sea expeditions could make a vital contribution to these efforts. Indeed, genetic data could be gathered for several species covering a range of PLD values in order to corroborate the connectivity patterns simulated here between seamounts. In addition, behavioural data such as larval and adult mobility, and demographic data including egg production and pre- and post-settlement mortality, should also be considered, because these

572 factors are as critical information as connectivity in determining the dynamics of populations,

573 and therefore their persistence.

574

Fig. 1. Main currents of the SWIO obtained from OSCAR current data averaged over the period 2010–2017, and the location of the nine studied seamounts, the eight coastal sites and surrounding countries (buffers).

Fig. 2. Trajectories of drifters passing less than 50 km from (a) La Pérouse, (b) MAD-Ridge and (c) Walters Shoal during their drift in the SWIO. Small white circles show the closest locations of drifters to seamounts used as the start of the represented trajectories, and small black circles are the final locations.

Fig. 3. Connectivity matrices between all seamounts and coastal sites for PLDs of (a) 15, (b) 120 and (c) 360 d. The values represent the percentage of larvae released at each release site transported to each destination site at the given PLD. The cells in the diagonal of the matrices are values of local retention. White = no connectivity (0%). Note that the colour scale differs between panels.

Fig. 4. Connectivity matrices between seamounts and coastal ecosystems for PLDs of (a) 15, (b) 120 and (c) 360 d. The values represent the percentage of larvae released at each release site transported to each destination site at the given PLD. The cells in the diagonal of the matrices are values of local retention. White = no connectivity (0%). Note that the colour scale differs between panels.

Fig. 5. Maps of average density for virtual larvae released at La Pérouse (a, d, g), MAD-Ridge (b, e, h) and Walters Shoal (c, f, i) for PLDs of 15, 120 and 360 d. Pink dots are the locations

598 of the drifters shown in Figure 2 at the same time (i.e. 15, 120 and 360 d after they passed less
599 than 50 km from the seamount).
600
601 Fig. 6. Local retention (%) at La Pérouse, MAD-Ridge and Walters Shoal for PLDs of 15, 30,
602 45, 90, 120 180, 270 and 360 d.
603
604 Fig. 7. Connectivity (%) between La Pérouse, MAD-Ridge and Walters Shoal for PLDs of 15,
605 30, 45, 90, 120, 180, 270 and 360 d.
606
607 Fig. 8. Origin of the larvae reaching La Pérouse, MAD-Ridge and Walters Shoal for PLDs of
608 (a) 15, (b) 120 and (c) 360 d.
609
610 Fig. 9. Maps of average density for virtual larvae released at all seamounts and coastal sites
611 for PLDs of (a) 30, (b) 45 and (c) 90 d. These PLD correspond broadly to labrid and *Apogon*
612 *spp*., *Synodus* sp., and the acanthurid *Naso* sp., respectively.
613
614 Fig. 10. Origin of larvae reaching MAD-Ridge (imports) for PLDs of (a) 30, (b) 45 and (c) 90
615 d, and the destination of larvae leaving MAD-Ridge (exports) for PLDs of (d) 30, (e) 45 and
616 (f) 90 d. These PLD correspond broadly to labrid and *Apogon* spp., *Synodus* sp., and
617 acanthurid *Naso* sp., respectively.
618
619 Fig. 11. Age distributions of virtual larvae arriving at MAD-Ridge from (a) Fort Dauphin and
620 (b) Mamanjary, and arriving at La Pérouse from (c) La Saline and (d) Morne Brabant.
621

622 Table 1. Mean distances of larval dispersal (km) from each seamount for different Pelagic

623 Larval Durations (PLDs).

FROM \ PLD	15	30	45	60	90	120	180	270	360
La Pérouse	*167*	*283*	*355*	*423*	*540*	*628*	*793*	*1031*	*1284*
MAD-Ridge	*337*	*460*	*575*	*665*	*804*	*901*	*1086*	*1368*	*1544*
Walters Shoal	*109*	*217*	*296*	*348*	*439*	*517*	*678*	*869*	*1014*
Atlantis Bank	*125*	*211*	*266*	*302*	*370*	*431*	*542*	*699*	*844*
Sapmer Bank	*164*	*236*	*292*	*356*	*443*	*530*	*674*	*854*	*1027*
Middle of What Seamount	*205*	*348*	*473*	*555*	*664*	*754*	*891*	*1061*	*1233*
Coral Seamount	*342*	*605*	*847*	*1070*	*1459*	*1718*	*2086*	*2393*	*2587*
Melville Bank	*311*	*551*	*719*	*830*	*979*	*1080*	*1256*	*1465*	*1638*
Un-named Seamount	*195*	*279*	*394*	*452*	*523*	*622*	*782*	*974*	*1122*
Mean	**217**	**354**	**469**	**556**	**691**	**798**	**976**	**1190**	**1366**

624

625

Appendix Fig. A. Trajectories of drifters passing <100 km from (a) La Pérouse, (b) MAD-Ridge and (c) Walters Shoal during their drift in the SWIO. Small white circles show the closest locations of drifters to seamounts used as the start of the represented trajectories, and small black circles are the final locations.

Appendix Fig. B. Connectivity matrices between all seamounts and coastal sites for PLDs of (a) 30, (b) 45, (c) 60, (d) 90, (e) 180 and (f) 270 d. The values represent the percentage of larvae released at each release site transported to each destination site at the given PLD. The cells in the diagonal of the matrices are values of local retention. White = no connectivity (0%). Note that the colour scale differs between panels.

Appendix Fig. C. Variability (seasonal and interannual combined) of simulated connectivity for PLDs of (a) 15, (b) 120 and (c) 360 d. CV is the relative standard deviation (ratio of the standard deviation to the mean).

Appendix Fig. D. Connectivity matrices between seamounts and coastal ecosystems for PLDs of (a) 30, (b) 45, (c) 60, (d) 90, (e) 180 and (f) 270 d. The values represent the percentage of larvae released at each release site and transported to each destination site at the given PLD. The cells in the diagonal of the matrices are values of local retention. White = no connectivity (0%). Note that the colour scale differs between panels.

Appendix Fig. E. Connectivity matrices between all seamounts and coastal sites for all PLDs. The buffer used around all release and destination sites was 1° (instead of the 1/3° in Fig. 3 and Appendix Fig. B). The values represent the percentage of larvae released at each release site transported to each destination site at the given PLD. The cells in the diagonal of the

651 matrices are values of local retention. White = no connectivity (0%). Note that the colour
652 scale differs between panels.

653

References

Alekseeva, E.I., 1983. Maturation of ovaries, nature of spawning and local specific character of genital cycles of alfonsino *Beryx splendens* Lowe from the Atlantic Ocean. In: Problems of early ontogeny of fish – theses of reports, pp. 72–73. Kaliningrad, USSR, AtlantNIRO (in Russian).

Amemou, H., Koné, V., Aman, A., Lett, C. (submitted) Assessment of a Lagrangian model using trajectories of oceanographic drifters and fishing devices in the Tropical Atlantic Ocean. Prog. Oceanogr.

Andrello, M., Guilhaumon, F., Albouy, C., Parravicini, V., Scholtens, J., Verley, P., Barange, M., Sumaila, U.R., Manel, S., Mouillot, D., 2017. Global mismatch between fishing dependency and larval supply from marine reserves. Nature Comms 8, 16039.

Andrello, M., Mouillot, D., Beuvier, J., Albouy, C., Thuiller, W., Manel, S.. 2013. Low connectivity between Mediterranean Marine Protected Areas: a biophysical modeling approach for the dusky grouper Epinephelus marginatus. PLoS ONE 8, e68564.

Annasawmy, P., Ternon, J-F., Cotel, P., Cherel, Y., Romanov, E.V., Roudaut, G., Lebourges-Dhaussy, A., Ménard, F., Marsac, F., 2019. Micronekton distributions and assemblages at two shallow seamounts of the south-western Indian Ocean: Insights from acoustics and mesopelagic trawl data, Prog. Oceanogr. 178, 102161. doi:10.1016/j.pocean.2019.102161

Annasawmy, P., Ternon, J-F., Lebourges-Dhaussy, A., Roudaut, G., Herbette, S., Ménard, F., Cotel, P., Marsac, F., 2020. Micronekton distribution as influenced by mesoscale eddies, Madagascar shelf and shallow seamounts in the south-western Indian Ocean: an acoustic approach. Deep-Sea Res. II. (this issue).

Armsworth, P.R. 2002. Recruitment limitation, population regulation, and larval connectivity in reef fish metapopulations. Ecology 83, 1092–1104.

Boehlert, G.W., Watson, W., Sun, L.C., 1992. Horizontal and vertical distributions of larval fishes around an isolated oceanic island in the tropical Pacific. Deep Sea Res. A. Oceanographic Research Papers, 39(3–4), 439-466.

Bonjean, F., Lagerloef, G.S.E., 2002. Diagnostic model and analysis of the surface currents in the tropical Pacific Ocean. J. Phys. Oceanogr. 32(10), 2938-2954.

Booth, J.D., 2006. *Jasus* species. In: Phillips B.F. (ed.) Lobsters: Biology, Management, Aquaculture and Fisheries. Blackwell Scientific, Oxford, pp 340–358.

Bryan-Brown, D.N., Brown, C.J., Hughes, J.M., Connolly, R.M., 2018. Patterns and trends in marine population connectivity research. Mar. Ecol. Prog. Ser. 585, 243–256. https://doi.org/10.3354/meps12418

Burgess, S.C., Nickols, K.J., Griesemer, C.D., Barnett, L.A., Dedrick, A.G., Satterthwaite, E.V., et al., 2014. Beyond connectivity: how empirical methods can quantify population persistence to improve marine protected-area design. Ecol. Appl. 24, 257–270. doi: 10.1890/13-0710.1.

Chapman, P., Marco, S.F.D., Davis, R., Coward, A., 2003. Flow at intermediate depths around Madagascar based on ALACE float trajectories. Deep Sea Res. II: Topical Studies in Oceanography 50, 1957–1986. doi:10.1016/S0967-0645(03)00040-7

Cherel, Y., Romanov, E.V., Annasawmy, P., Thibault, D., Ménard, F., 2020. Micronektonic fish species over three seamounts in the southwestern Indian Ocean. Deep-Sea Res. II. (this issue).

Cherubin, L.M., Nemeth, R.S., Idrisi, N., 2011. Flow and transport characteristics at an *Epinephelus guttatus* (red hind grouper) spawning aggregation site in St Thomas (US Virgin Islands). Ecol. Model. 222, 3132–3148. doi:10.1016/j.ecolmodel.2011.05.031

Cinner, J.E., Huchery, C., MacNeil, M.A., Graham, N.A.J., McClanahan, T.R., Maina, J., et al., 2016. Bright spots among the world's coral reefs. Nature 535, 416–419.

Clark, M.R., Schlacher, T.., Rowden, A.A., Stocks, K.I., Consalvey, M., 2012. Science priorities for seamounts: research links to conservation and management. PLoS ONE 7, e29232, doi:10.1371.

Cowen, R.K., 2002. Larval dispersal and retention and consequences for population connectivity. In: Sale, P.F. (ed.), Coral Reef Fishes: Dynamics and Diversity in a Complex Ecosystem. Academic Press, London. pp. 149–170.

Cowen, R.K., Gawarkiewicz, G., Pineda, J., Thorrold, S., Werner, F., 2007. Population connectivity in marine systems: an overview. Oceanography 20, 14–21. https://doi.org/10.5670/oceanog.2007.26.

Cowen, R.K., Lwiza, K.M.M., Sponaugle, S., Paris, C.B., Olson, D.B., 2000. Connectivity of marine populations: open or closed? Science 287, 857.

Crochelet, E., Chabanet, P., Pothin, K., Lagabrielle, E., Roberts, J., Pennober, G., Lecomte-Finiger, R. and Petit, M., 2013. Validation of a fish larvae dispersal model with otolith data in the western Indian Ocean and implications for marine spatial planning in data-poor regions. Ocean Coast. Mgmt 86, pp.13-21.

Crochelet, E., Roberts, J., Lagabrielle, E., Obura, D., Petit, M., Chabanet, P., 2016. A model-based assessment of reef larvae dispersal in the Western Indian Ocean reveals regional connectivity patterns—potential implications for conservation policies. Reg Stud. Mar. Sci. 7, pp.159-167.

de Ruijter, W.P.M., van Aken, H.M., Beier, E.J., Lutjeharms, J.R.E., Matano, R.P., Schouten, M.W., Schlitzer, R., 2004. Eddies and dipoles around South Madagascar: formation, pathways and large-scale impact. Deep Sea Res. 51, 383-400.

Doherty, P. J., Planes, S., Mather, P., 1995. Gene flow and larval duration in seven species of fish from the Great Barrier Reef. Ecology, 76(8), 2373-2391.

Edgar, G.J., Stuart-Smith, R.D., Willis, T.J., Kininmonth, S., Baker, S.C., Banks, S., et al., 2014. Global conservation outcomes depend on marine protected areas with five key features. Nature 506, 216–220.

Faillettaz, R., Paris, C.B., Irisson, J-O., 2018. Larval fish swimming behavior alters dispersal patterns from Marine Protected Areas in the North-Western Mediterranean Sea. Front. Mar. Sci. 5, 97. doi: 10.3389/fmars.2018.00097

FAO, 2018. The State of World Fisheries and Aquaculture 2018 - Meeting the sustainable development goals. Rome, FAO.

FFEM, 2013. Note d'Engagement de Projet (NEP). Conservation et exploitation durable des écosystèmes de monts sous-marins et sources hydrothermales du Sud-Ouest de l'Océan Indien au-delà des zones de juridiction nationale. 67 pp.

Fisher, R., Leis, J.M., Clark, D.L., Wilson, S.K., 2005. Critical swimming speeds of late-stage coral reef fish larvae: variation within species, among species and between locations. Mar. Biol. 147, 1201-1212.

Gamoyo, M., Obura, D., Reason, C.J.C., 2019. Estimating connectivity through larval dispersal in the Western Indian Ocean. J. Geophys. Res. Biogeosci. 124, 2446–2459. https://doi.org/10.1029/2019JG005128

Groeneveld, J.C., Griffiths, C.L., van Dalsen, A.P., 2006. A new species of spiny lobster, *Palinurus barbarae* (Decapoda, Palinuridae) from Walters Shoals on the Madagascar Ridge. Crustaceana 79(7), 821-823.

Guinot, D., Richer de Forges, B., 1981. Crabes de profondeur, nouveaux ou rares, de l'Indo-Pacifique (Crustacea, Decapoda, Brachyura). Bulletin du Muséum national d'Histoire naturelle, 1ère partie 4(2), 1113-1153. 2ème partie 4(3), 227-260.

Guinotte, J., 2011. Seamount map of the Indian Ocean. Marine Conservation Biology Institute; 3 pp. http://www.savethehighseas.org/publicdocs/Indian-Ocean-map.pdf

Harris, S., Noyon, M., Roberts, M.J., Marsac, F., 2020. Ichthyoplankton assemblages at three shallow seamounts in the South West Indian Ocean: La Pérouse, MAD-Ridge and Walters Shoal. Deep-Sea Res. II. (this issue).

Hastings, A., Botsford, L.W., 2006. Persistence of spatial populations depends on returning home. Proc. Natl Acad. Sci. 103, 6067–6072. doi: 10.1073/pnas.0506651103 PMID: 16608913

Hellberg, M.E., 2007. Footprints on water: the genetic wake of dispersal among reefs. Coral Reefs 26, 463–473.

Irisson, J.O., Paris, C.B., Guigand, C.M., Planes, S., 2010. Vertical distribution and ontogenetic 'migration' in coral reef fish larvae. Limnol. Oceanogr. 55, 909-919.

Jones, G.P., Almany, G.R., Russ, G.R., Sale, P.F., Steneck, R.S., van Oppen, M.J.H., et al., 2009. Larval retention and connectivity among populations of corals and reef fishes: history, advances and challenges. Coral Reefs 28, 307–325.

Kingsford, M.J., Leis, J.M., Shanks, A., Lindeman, K.C., Morgan, S.G., Pineda, J., 2002. Sensory environments, larval abilities and local self-recruitment. Bull. Mar. Sci. 70, 309–340.

Koslow, J.A., Boehlert, G.W., Gordon, J.D.M., Haedrich, R.L., Lorance, P., Parin, N., 2000. Continental slope and deep-sea fisheries: implications for a fragile ecosystem. ICES J. Mar. Sci. 57, 548-557.

Leis, J.M., 1984. Larval fish dispersal and the east Pacific Barrier. Océanogr. Trop. 19, 181-192.

Leis, J.M., 1991. The pelagic phase of coral reef fishes: larval biology of coral reef fishes. pp. 183–230. In: Sale, P.F. (ed.). The Ecology of Fishes on Coral Reefs, Academic Press, San Diego. 754 pp.

Leis, J., 2002. Pacific coral-reef fishes: the implications of behaviour and ecology of larvae for biodiversity and conservation, and a reassessment of the open population paradigm. Env. Biol. Fish. 65, 199–208.

Leis, J., 2010. Ontogeny of behaviour in larvae of marine demersal fishes. Ichthyol. Res 57, 325–342. doi:10.1007/s10228-010-0177-z

Leis, J.M., Carson-Ewart, B.M., 2002. *In situ* settlement behaviour of damselfish (Pomacentridae) larvae. J. Fish Biol. 61, 325-346.

Lett, C., Verley, P., Mullon, C., Parada, C., Brochier, T., Penven, P., Blanke, B., 2008. A Lagrangian tool for modelling ichthyoplankton dynamics. Env. Model. Softw. 23, 1210–1214. doi:10.1016/j.envsoft.2008.02.005

Liu, Y., Weisberg, R.H., Vignudelli, S., Mitchum, G.T., 2014. Evaluation of altimetry-derived surface current products using Lagrangian drifter trajectories in the eastern Gulf of Mexico. J. Geophys. Res.: Oceans 119, 2827–2842. https://doi.org/10.1002/2013JC009710.

Luiz, O.J., Allen, A.P., Robertson, D.R., Floeter, S.R., Kulbicki, M., Vigliola, L., Becheler, R., Madin, J.S., 2013. Adult and larval traits as determinants of geographic range size among tropical reef fishes. Proc. Nat. Acad. Sci., 110(41), 16498-16502. https://doi.org/10.1073/pnas.1304074110

Lumpkin, R., Centurioni, L., 2019. Global Drifter Program quality-controlled 6-hour interpolated data from ocean surface drifting buoys. NOAA National Centers for Environmental Information. Dataset. https://doi.org/10.25921/7ntx-z961.

Maina, J.M., Gamoyo, M., Adams, V.M., D'agata, S., Bosire, J., Francis, J., Waruinge, D., 2020. Aligning marine spatial conservation priorities with functional connectivity across maritime jurisdictions. Conserv. Sci. Practice. https://doi.org/10.1111/csp2.156

Manel, S., Loiseau, N., Andrello, M., Fietz, K., Goñi, R., Forcada, A., Lenfant, P., Kininmonth, S., Marcos, C., Marques, V., Mallol, S., Pérez-Ruzafa, A., Breusing, C., Puebla, O., Mouillot, D., 2019. Long-distance benefits of marine reserves: myth or reality? Trends Ecol. Evol. 34, 342–354. https://doi.org/10.1016/j.tree.2019.01.002

Marsac, F., Annasawmy, P., Noyon, M., Demarcq, H., Soria, M., Rabearisoa, N., Bach, P., Cherel, Y., Grelet, J., Romanov, E.V. Physical environment and ecological interactions at and near La Pérouse seamount, northwest of Réunion Island, Indian Ocean. Deep Sea Res. II (this issue).

Mattio, L., Zubia, M., Loveday, B., Crochelet, E., Duong, N., Payri, C.E., Bhagooli, R., Bolton, J.J., 2013. Sargassum (Fucales, Phaeophyceae) in Mauritius and Réunion, western Indian Ocean: taxonomic revision and biogeography using hydrodynamic dispersal models. Phycologia 52, 578–594. https://doi.org/10.2216/13-150.1

Moberg, F., Folke, C., 1999. Ecological goods and services of coral reef ecosystems. Ecol. Econ. 29, 215–233.

Mora, C., Treml, E.A., Roberts, J., Crosby, K., Roy, D., Tittensor, D.P., 2012. High connectivity among habitats precludes the relationship between dispersal and range size in tropical reef fishes. Ecography 35, 89–96. doi:10.1111/j.1600-0587.2011.06874.x

Morato, T., Cheung, W.W.L., Pitcher T.J., 2004. Addition to Froese and Sampang's checklist of seamount fishes. In: Morato, T., Pauly, D. (eds). Seamounts: Biodiversity and Fisheries. Fisheries Centre Research Reports, 12 (5), Appendix 1: 1-6. Fisheries Centre, University of British Columbia, Canada.

Obura, D., 2012. The diversity and biogeography of Western Indian Ocean reef-building corals. PLoS ONE 7(9), e45013. https://doi.org/10.1371/journal.pone.0045013

Peliz, A., Marchesiello, P., Dubert, J., Marta-Almeida, M., Roy, C., Queiroga, H., 2007. A study of crab larvae dispersal on the western Iberian Shelf: physical processes. J. Mar. Syst. 68, 215–236.

Pineda, J., Reyns, N.B., Starczak, V.R., 2009. Complexity and simplification in understanding recruitment in benthic populations. Pop. Ecol. 51, 17–32. DOI: 10.1007/s10144-008-0118-0

Planes, S., Doherty, P.J., Bernardi, G., 2001. Strong genetic divergence among populations of a marine fish with limited dispersal, *Acanthochromis polyacanthus*, within the Great Barrier Reef and the Coral Sea. Evolution 55, 2263-2273.

Pollard, R., Read, J., 2017. Circulation, stratification and seamounts in the Southwest Indian Ocean. Deep Sea Res. Part II. Top. Stud. Oceanogr. 136, 36–43. https://doi.org/10.1016/j.dsr2.2015.02.018.

Popova, E., Vousden, D., Sauer, W.H., Mohammed, E.Y., Allain, V., Downey-Breedt, N., Fletcher, R., Gjerde, K.M., Halpin, P.N., Kelly, S., Obura, D., 2019. Ecological connectivity between the areas beyond national jurisdiction and coastal waters: safeguarding interests of coastal communities in developing countries. Mar. Pol. 104, 90-102.

Pous, S., Feunteun, E., Ellien, C., 2010. Investigation of tropical eel spawning area in the South-Western Indian Ocean: influence of the oceanic circulation. Prog. Oceanogr. 86, 396–413. https://doi.org/10.1016/j.pocean.2010.06.002.

Read, J., Pollard, R., 2017. An introduction to the physical oceanography of six seamounts in the southwest Indian Ocean. Deep Sea Res. II: Topical Studies in Oceanography 136, 44–58. https://doi.org/10.1016/j.dsr2.2015.06.022.

Reid, K., Crochelet, E., Bloomer, P., Hoareau, T.B., 2016. Investigating the origin of vagrant dusky groupers, Epinephelus marginatus (Lowe, 1834), in coastal waters of Réunion Island. Mol. Phylogen. Evol. 103, 98-103.

Riginos, C., Victor, B.C., 2001. Larval spatial distributions and other early life–history characteristics predict genetic differentiation in eastern Pacific blennioid fishes. Proc. R. Soc. Lond.. Series B: Biological Sciences, 268(1479), 1931-1936.

Roberts, C.M., 1997. Connectivity and management of Caribbean coral reefs. Science 278, 1454–1457. doi:10.1126/science.278.5342.1454

Roberts, M.J., Ternon, J-F., Marsac, F., Noyon, M., 2020. The MAD-Ridge Project: bio-physical coupling around a shallow seamount on the northern Madagascar Ridge, Southwest Indian Ocean. Deep-Sea Res. II. (this issue).

Rogers, A.D., 2012. An Ecosystem Approach to Management of Seamounts in the Southern Indian Ocean. 1. Overview of Seamount Ecosystems and Biodiversity. IUCN, Gland, Switzerland. 60 pp.

Rogers, A.D., Alvheim, O., Bemanaja, E., Benivary, D., Boersch-Supan, P., Bornman, T.G., Cedras, R., Du Plessis, N., Gotheil, S., Høines, A., Kemp, K., Kristiansen, J., Letessier, T., Mangar, V., Mazungula, N., Mørk, T., Pinet, P., Pollard, R., Read, J., Sonnekus, T., 2017. Pelagic communities of the South West Indian Ocean seamounts: R/V Dr Fridtjof Nansen Cruise 2009-410. Deep-Sea Res. II: Topical Studies in Oceanography 136, 5–35. doi:10.1016/j.dsr2.2016.12.010

Romanov, E.V., 2003. Summary and review of Soviet and Ukrainian scientific and commercial fishing operations on the deepwater ridges of the Southern Indian Ocean. In: Romanov, E.V. (ed.). FAO Fish. Circ. 991, 84 pp.

Rowden, A.A., Dower, J.F., Schlacher, T.A., Consalvey, M., Clark, M.R., 2010. Paradigms in seamount ecology: fact, fiction, and future. Mar. Ecol. 31(Suppl. 1), 226–239.

Schleyer, M.H., Downey-Breedt, N.J., Benayahu, Y., 2019. Species composition of Alcyonacea (Octocorallia) on coral reefs at Europa Island and associated connectivity across the Mozambique Channel. Mar. Biodiv. 49, 2485–2491. https://doi.org/10.1007/s12526-019-00975-7.

Schultz, E.T., Cowen, R.K., 1994. Recruitment of coral reef fishes to Bermuda: lLcal retention or long-distance transport? Mar. Ecol. Prog. Ser. 109, 15–28.

Selkoe, K.A., Toonen, R.J., 2011. Marine connectivity: a new look at pelagic larval duration and genetic metrics of dispersal. Mar. Ecol. Prog. Ser. 436, 291-305.

SIOFA, 2019. Report of the Fourth Session of the Scientific Committee (SC4), p. 195, 25- 29 March 2019, Yokohama.

Shotton, R., 2006. Management of demersal fisheries resources of the southern Indian Ocean. FAO Fish. Circ. 1020, 90 pp.

Shotton, R., 2016. Global review of alfonsino (*Beryx* spp.), their fisheries, biology and management. FAO Fish. Aquacult. Circ. C1084, 154 pp.

Sikhakolli, R., Sharma, R., Basu, S., Gohil, B.S., Sarkar, A., Prasad, K.V.S.R., 2013. Evaluation of OSCAR ocean surface current product in the tropical Indian Ocean using in situ data. J. Earth Syst. Sci. 122, 187–199. doi:10.1007/s12040-012-0258-7

Stier, A.C., Hein, A.N., Parravicini, V., Kulbicki, M., 2014. Larval dispersal drives trophic structure across Pacific coral reefs. Nat. Comms, doi: 10.1038/ncomms6575

Tolimieri, N., Jeffs, A., Montgomery, J., 2000. Ambient sound as a cue for navigation by the pelagic larvae of reef fishes. Mar. Ecol. Prog. Ser. 207, 219–224. doi:10.3354/meps207219

Tomczak, M., Godfrey, J.S., 2003. Regional Oceanography: an Introduction, 2nd edn. Daya Publishing House, Delhi. 390 pp.

Treml, E.A., Halpin, P.N., Urban, D.L., Pratson, L.F., 2008. Modeling population connectivity by ocean currents, a graph-theoretic approach for marine conservation. Landscape Ecol. 23, 19–36.

UNEP-Nairobi Convention and WIOMSA (2015). The Regional State of the Coast Report: Western Indian Ocean. UNEP and WIOMSA, Nairobi, Kenya, 546 pp.

Van der Stocken, T., Menemenlis, D., 2017. Modelling mangrove propagule dispersal trajectories using high-resolution estimates of ocean surface winds and currents, Biotropica 49, 472–481. https://doi.org/10.1111/btp.12440.

Vianello, P., Herbette, S., Ternon, J-F., Demarcq, H., Roberts, M.J., 2020. Circulation and hydrography in the vicinity of a shallow seamount on the northern Madagascar Ridge. Deep-Sea Res. II. (this issue).

Victor, B.C., 1987. Growth, dispersal, and identification of planktonic labrid and pomacentrid reef-fish larvae in the eastern Pacific Ocean. Mar. Biol. 95, 145–152. doi:10.1007/BF00447496

Warner, R.R., Cowen, R.K., 2002. Local retention of production in marine populations: evidence, mechanisms, and consequences. Bull. Mar. Sci. 70, 245-249.

Zucchi, S., Ternon, J-F., Demarcq, H., Ménard, F., Guduff, S., Spadone, A., 2018. Oasis for marine life. State of knowledge on seamounts and hydrothermal vents. IUCN, Gland,

996 Switzerland, vi + 50 pp. ISBN: 978-2-8317-1934-4 (PDF). DOI:
997 10.2305/IUCN.CH.2018.14.en-fr
998

Formatting of funding sources

This work was partly carried out in the framework of the project P00917 entitled "Conservation and sustainable exploitation of seamount and hydrothermal wind ecosystems of the South West Indian Ocean in areas beyond national jurisdiction", funded by the French Global Environment Facility (FFEM), and conducted from 2014 to 2018.

Table 1. Mean distances of larval dispersal (km) from each seamount for different Pelagic Larval Durations (PLDs).

FROM \ PLD	**15**	**30**	**45**	**60**	**90**	**120**	**180**	**270**	**360**
La Perouse	*167*	*283*	*355*	*423*	*540*	*628*	*793*	*1031*	*1284*
MAD-Ridge	*337*	*460*	*575*	*665*	*804*	*901*	*1086*	*1368*	*1544*
Walters Shoal	*109*	*217*	*296*	*348*	*439*	*517*	*678*	*869*	*1014*
Atlantis Bank	*125*	*211*	*266*	*302*	*370*	*431*	*542*	*699*	*844*
Sapmer Bank	*164*	*236*	*292*	*356*	*443*	*530*	*674*	*854*	*1027*
Middle of What Seamount	*205*	*348*	*473*	*555*	*664*	*754*	*891*	*1061*	*1233*
Coral Seamount	*342*	*605*	*847*	*1070*	*1459*	*1718*	*2086*	*2393*	*2587*
Melville Bank	*311*	*551*	*719*	*830*	*979*	*1080*	*1256*	*1465*	*1638*
Un-named Seamount	*195*	*279*	*394*	*452*	*523*	*622*	*782*	*974*	*1122*
Mean	**217**	**354**	**469**	**556**	**691**	**798**	**976**	**1190**	**1366**

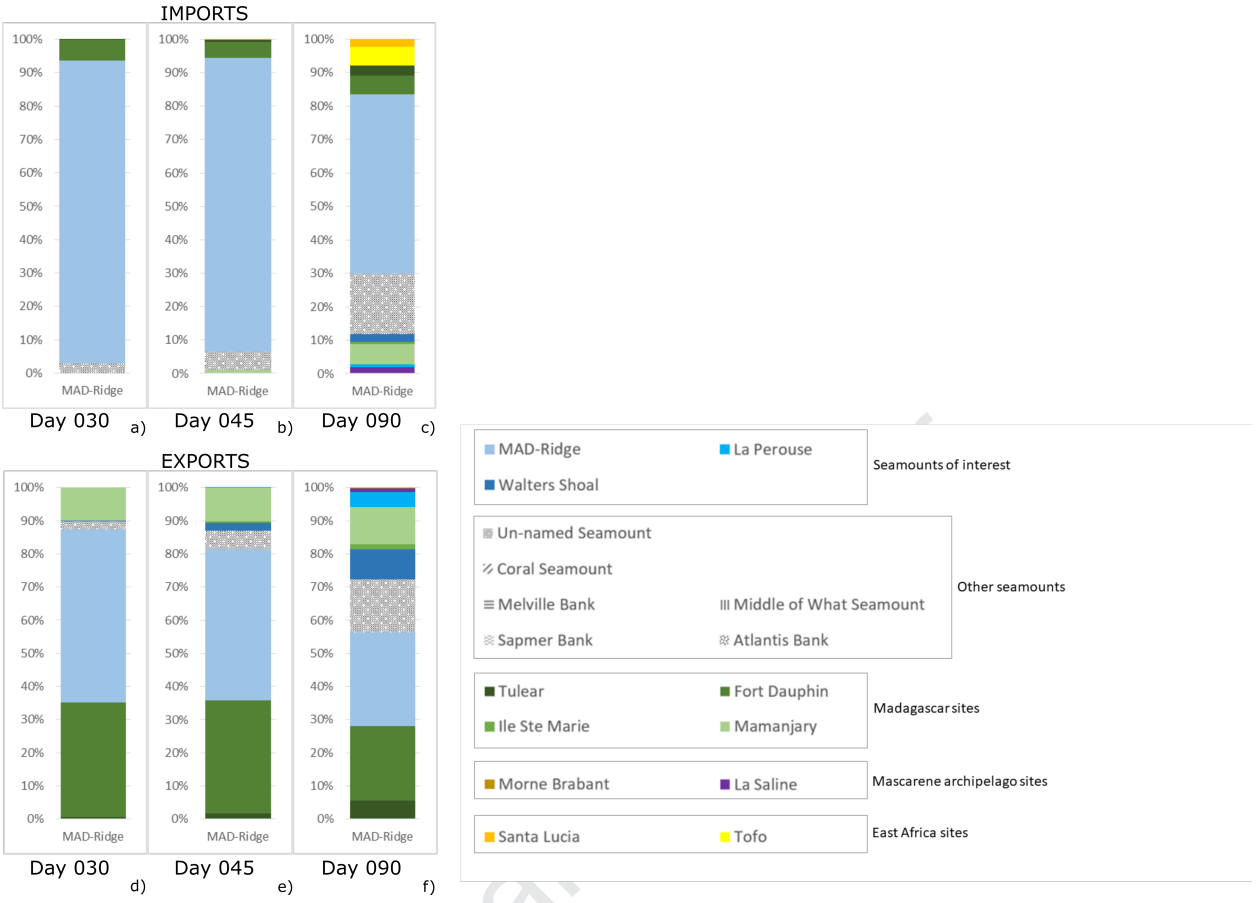
IMPORTS
100%
90%
80%
70%
60%
50%
40%
30%
20%
10%
0%
MAD-Ridge
Day 030
a)
Day 045
b)
Day 090
c)
EXPORTS
Day 030
d)
Day 045
e)
Day 090
f)
MAD-Ridge
La Perouse
Walters Shoal
Seamounts of interest
Un-named Seamount
Coral Seamount
Melville Bank
Middle of What Seamount
Sapmer Bank
Atlantis Bank
Other seamounts
Tulear
Fort Dauphin
Ile Ste Marie
Mamanjary
Madagascar sites
Morne Brabant
La Saline
Mascarene archipelago sites
Santa Lucia
Tofo
East Africa sites

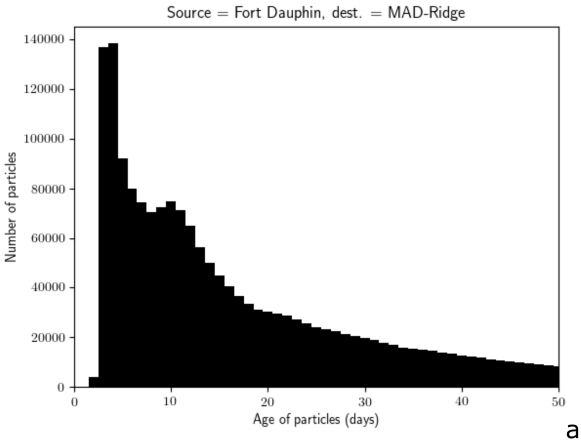
Source = Fort Dauphin, dest. = MAD-Ridge
Number of particles
Age of particles (days)
0
20000
40000
60000
80000
100000
120000
140000
0
10
20
30
40
50

a)

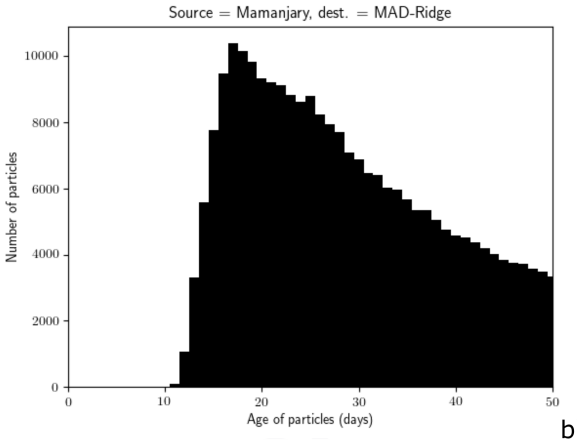
Source = Mamanjary, dest. = MAD-Ridge
Number of particles
Age of particles (days)
0
2000
4000
6000
8000
10000
0
10
20
30
40
50

b)

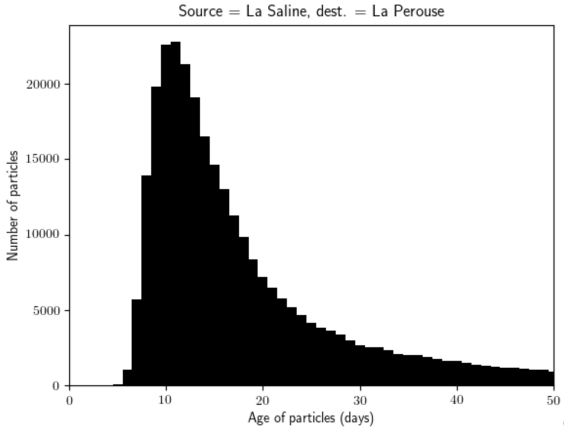
Source = La Saline, dest. = La Perouse
Number of particles
Age of particles (days)
0
5000
10000
15000
20000
0
10
20
30
40
50

c)

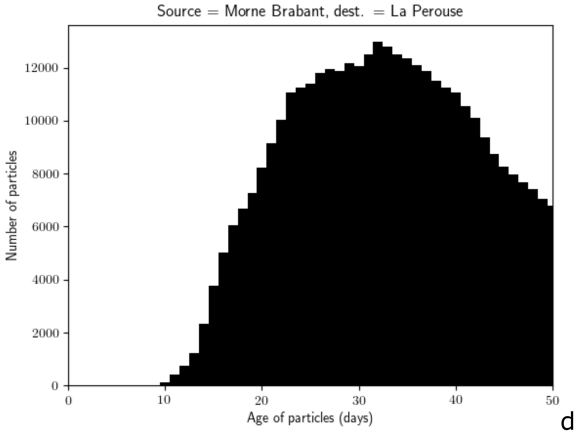
Source = Morne Brabant, dest. = La Perouse
Number of particles
Age of particles (days)
0
2000
4000
6000
8000
10000
12000
0
10
20
30
40
50

d)

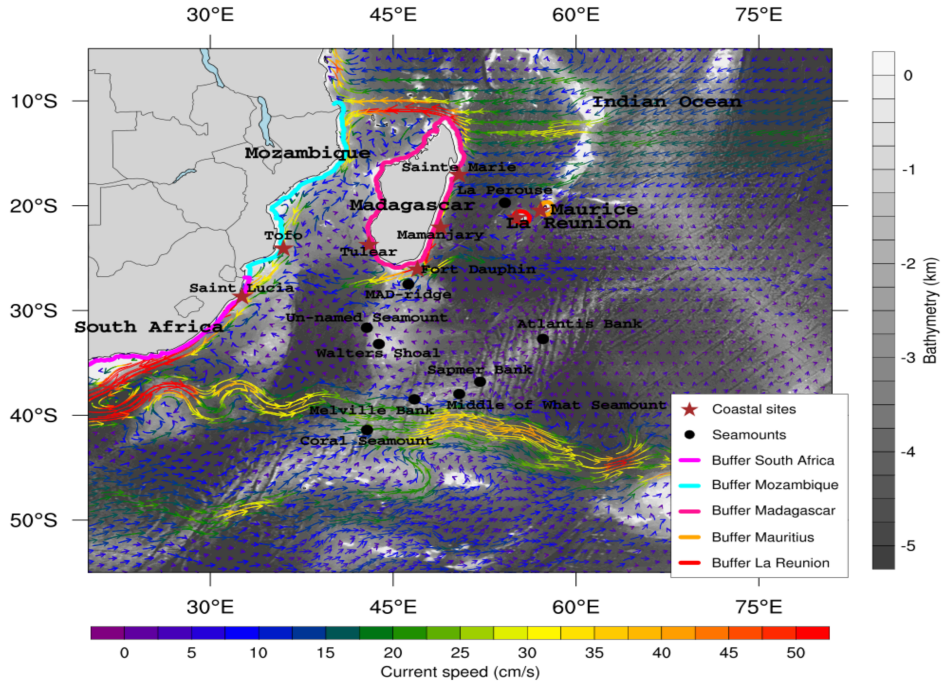

Name	**Summit depth (meters)**
Atlantis Bank	690
Sapmer Bank	261
Middle of What Seamount	876
Coral Seamount	175
Melville Bank	91
Un-named Seamount	1249
Walter's Shoal	18
La Pérouse	55
MAD-Ridge	240

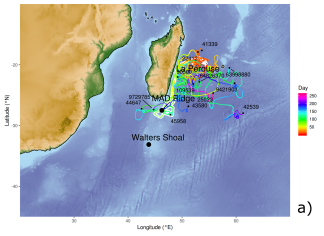

a)

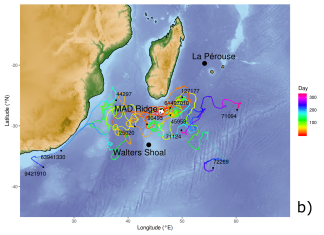

b)

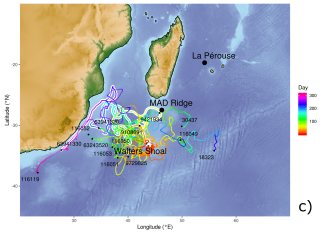

c)

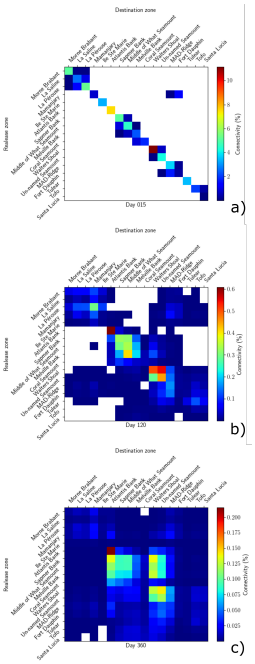

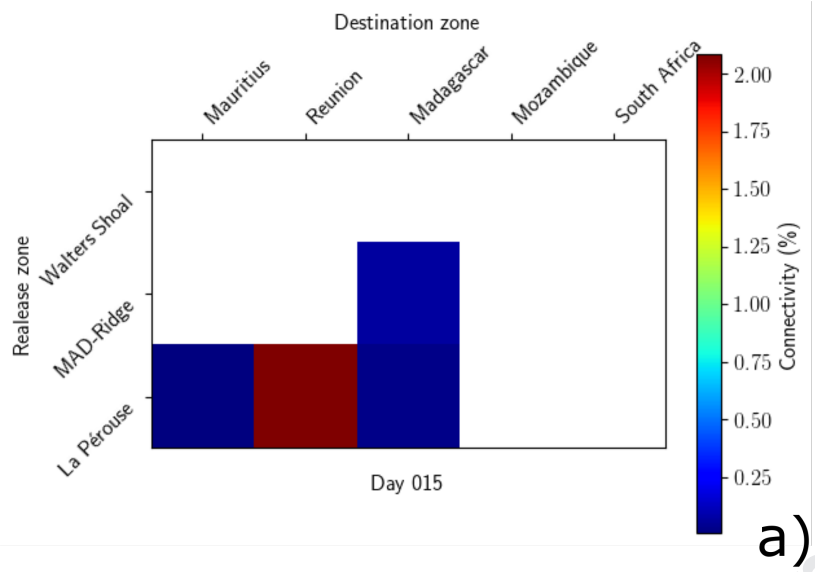
Destination zone
Mauritius
Reunion
Madagascar
Mozambique
South Africa
Realease zone
Walters Shoal
MAD-Ridge
La Pérouse
Day 015
Connectivity (%)
2.00
1.75
1.50
1.25
1.00
0.75
0.50
0.25

a)

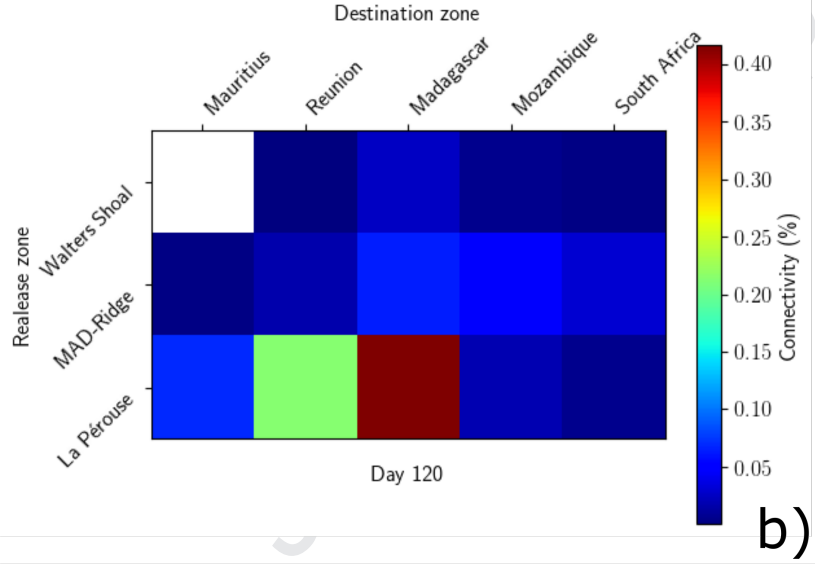
Destination zone
Mauritius
Reunion
Madagascar
Mozambique
South Africa
Realease zone
Walters Shoal
MAD-Ridge
La Pérouse
Day 120
Connectivity (%)
0.40
0.35
0.30
0.25
0.20
0.15
0.10
0.05

b)

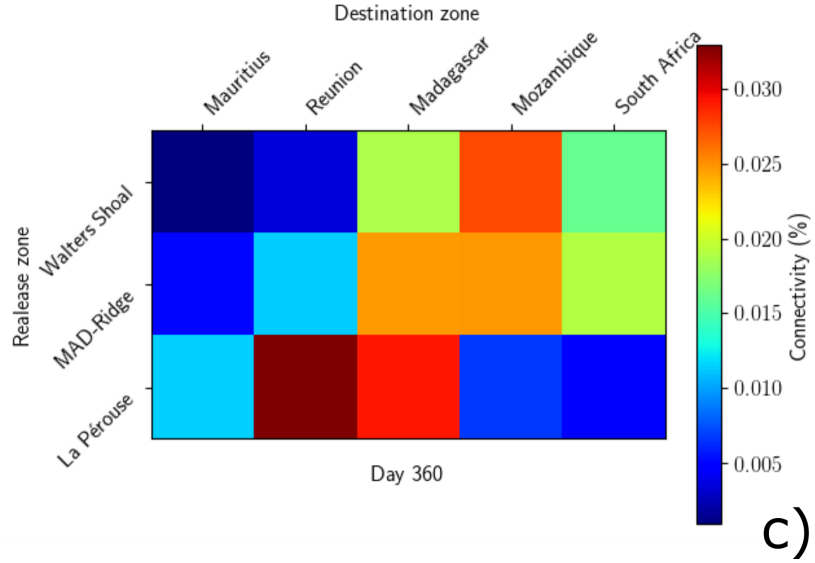
Destination zone
Mauritius
Reunion
Madagascar
Mozambique
South Africa
Realease zone
Walters Shoal
MAD-Ridge
La Pérouse
Day 360
Connectivity (%)
0.030
0.025
0.020
0.015
0.010
0.005

c)

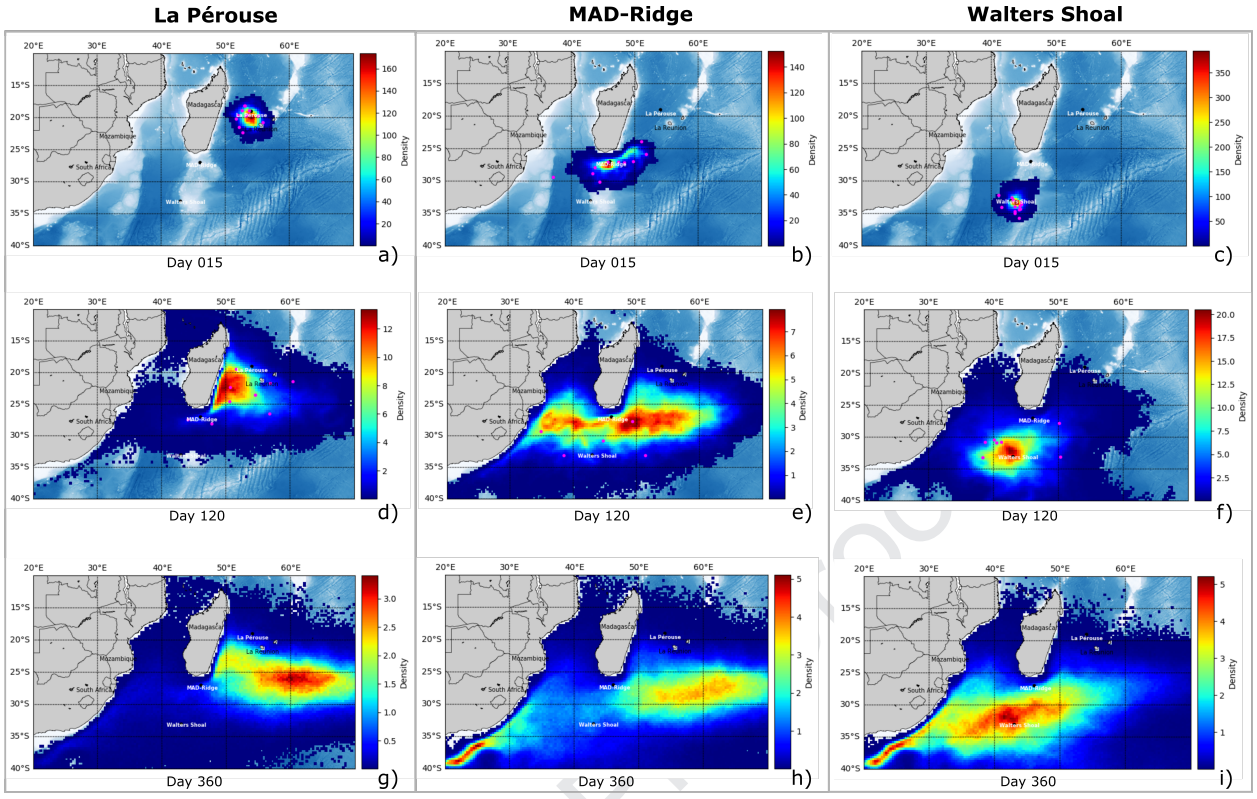

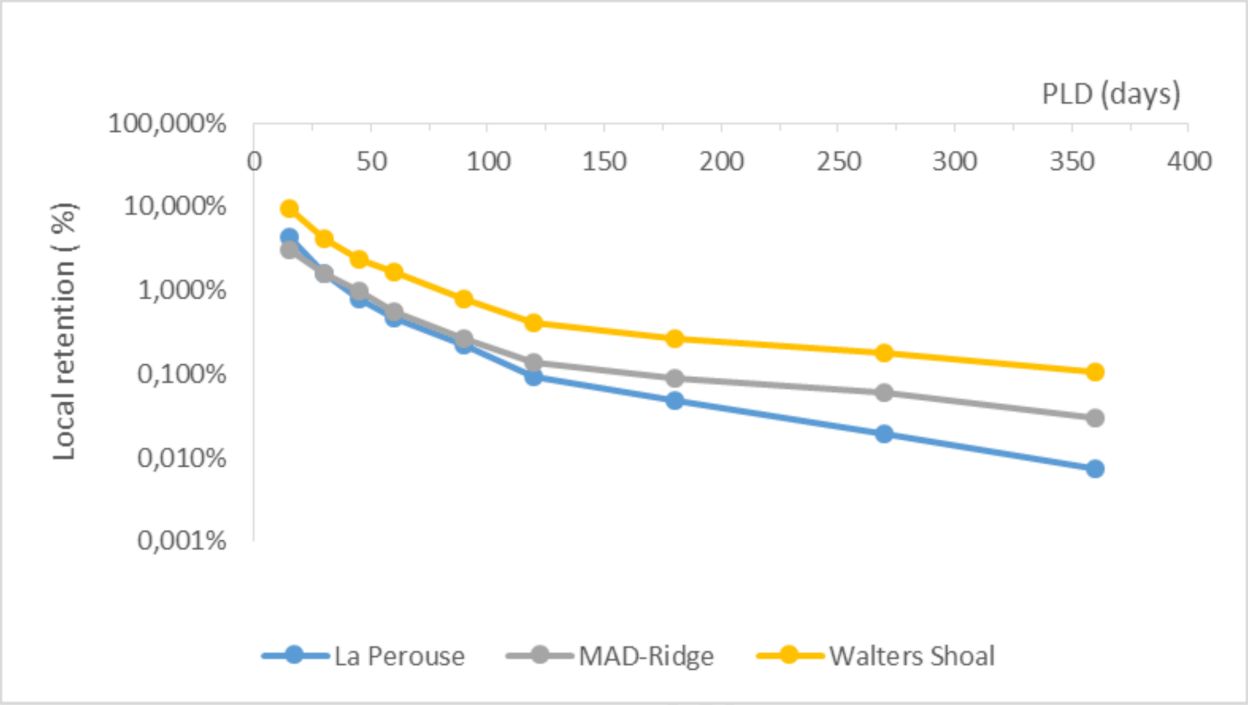
PLD (days)
100,000%
10,000%
1,000%
0,100%
0,010%
0,001%
Local retention (%)
0
50
100
150
200
250
300
350
400
La Perouse
MAD-Ridge
Walters Shoal

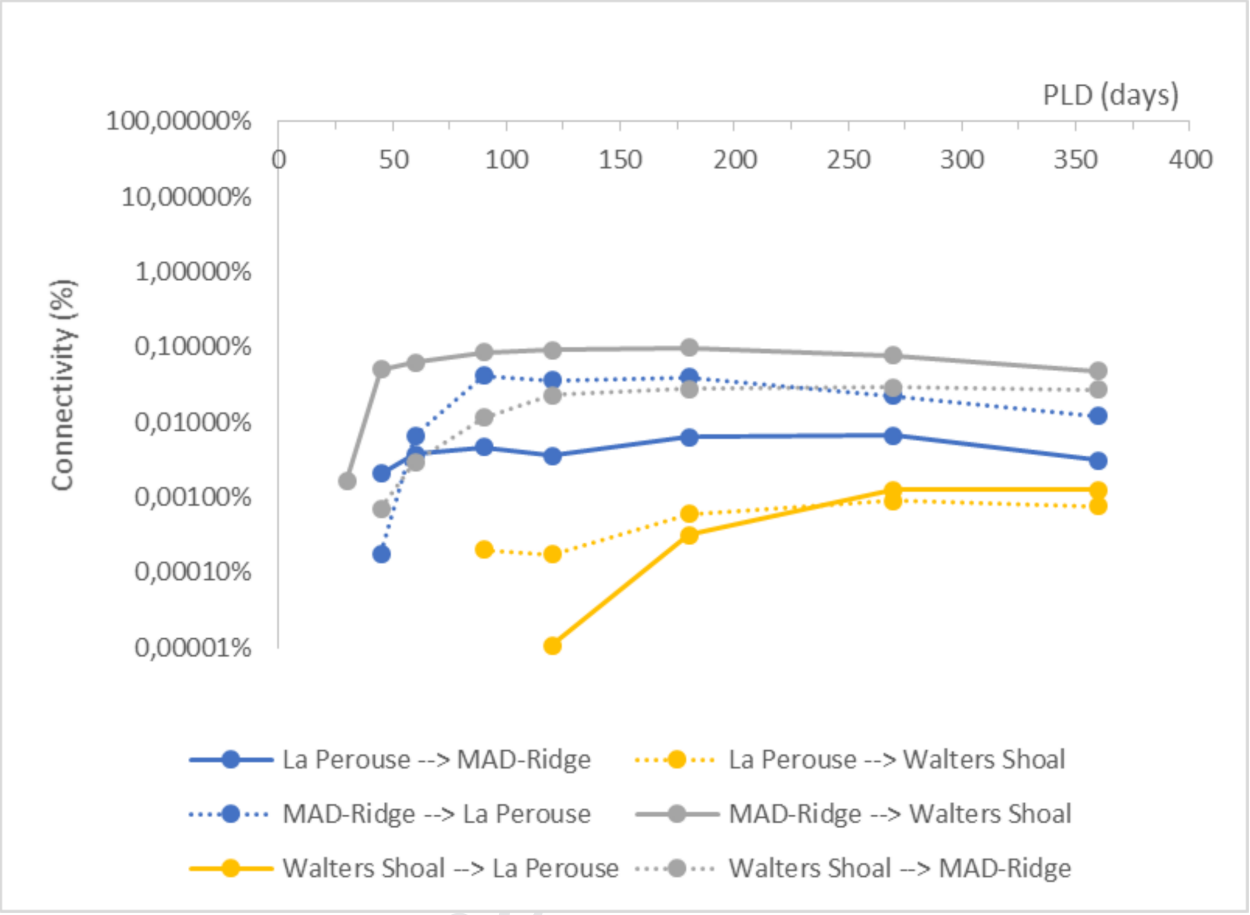
PLD (days)
100,00000%
10,00000%
1,00000%
0,10000%
0,01000%
0,00100%
0,00010%
0,00001%
Connectivity (%)
0
50
100
150
200
250
300
350
400
La Perouse --> MAD-Ridge
La Perouse --> Walters Shoal
MAD-Ridge --> La Perouse
MAD-Ridge --> Walters Shoal
Walters Shoal --> La Perouse
Walters Shoal --> MAD-Ridge

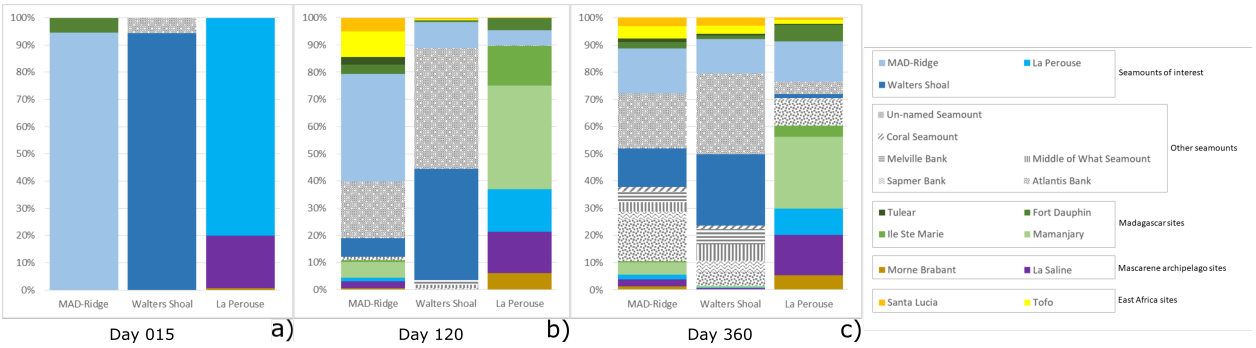

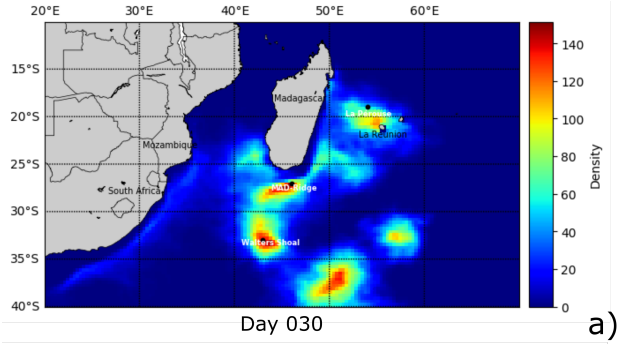

Day 030 a)

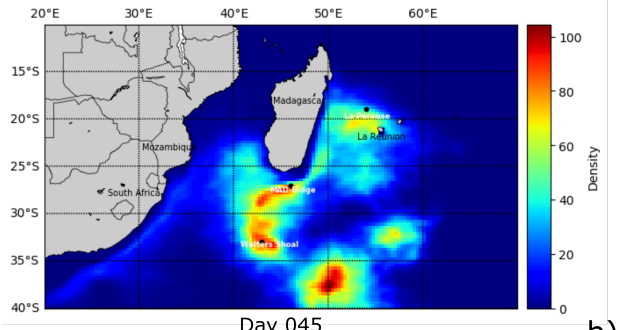

Day 045 b)

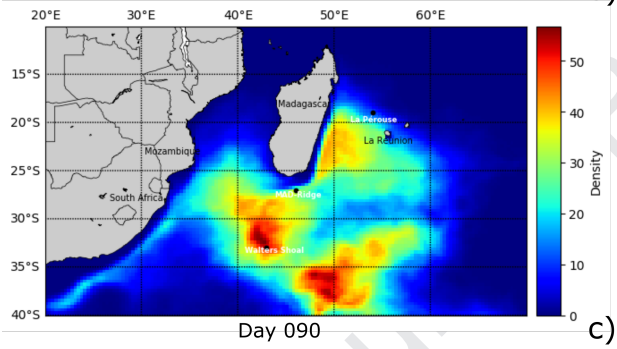

Day 090 c)

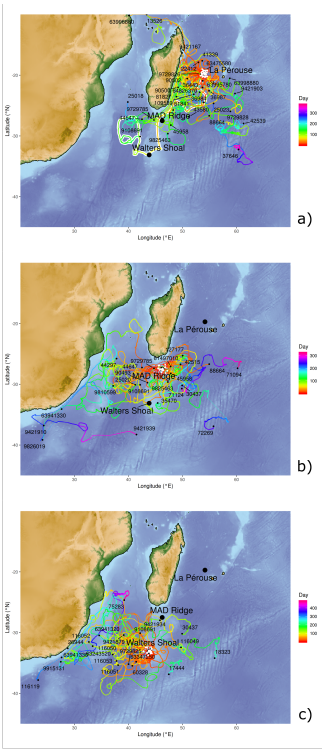

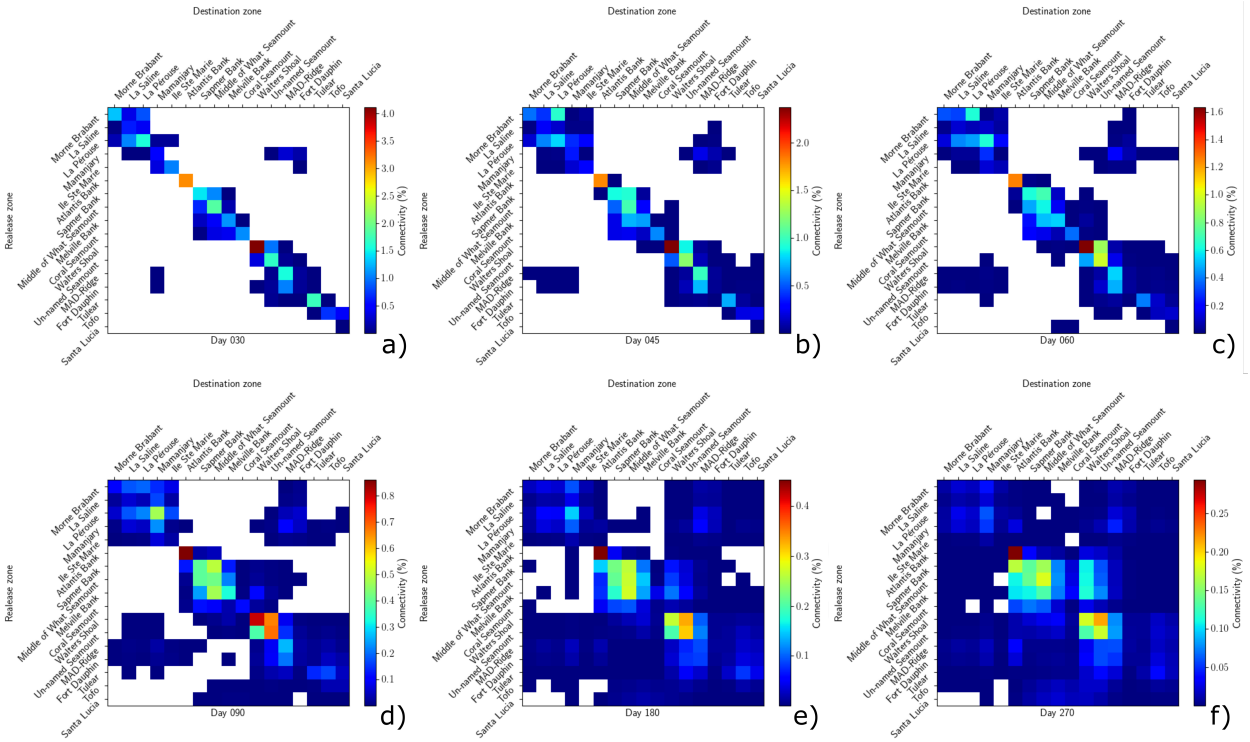

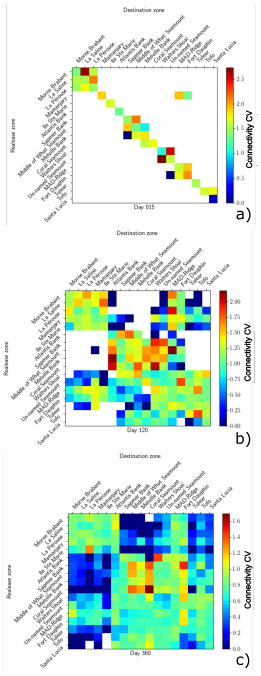

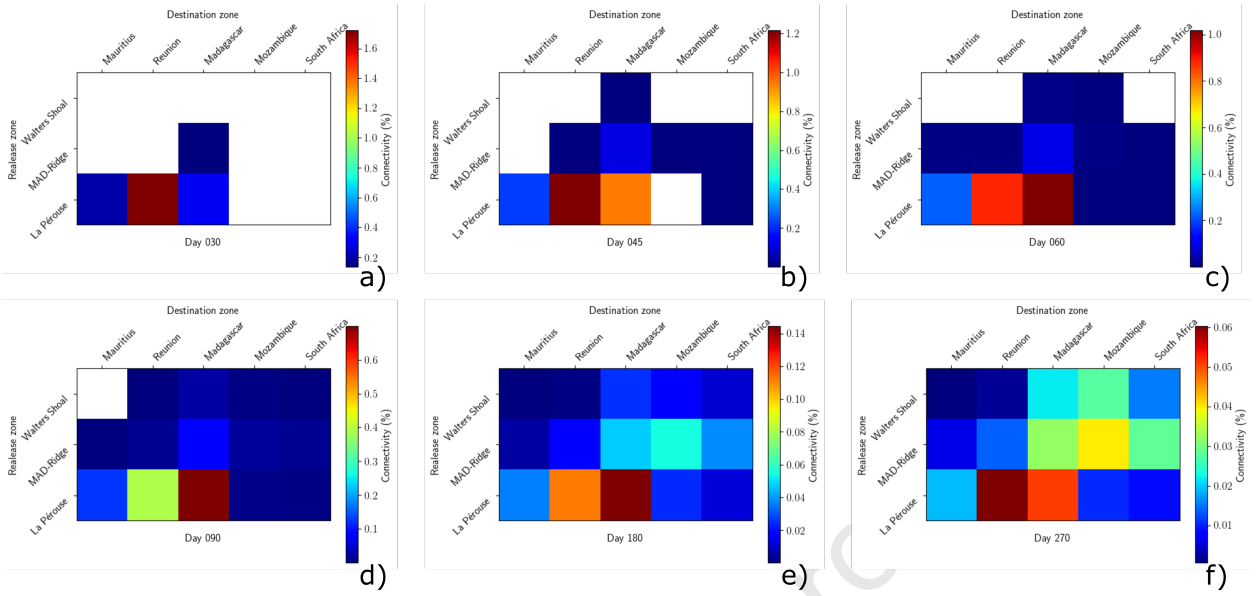

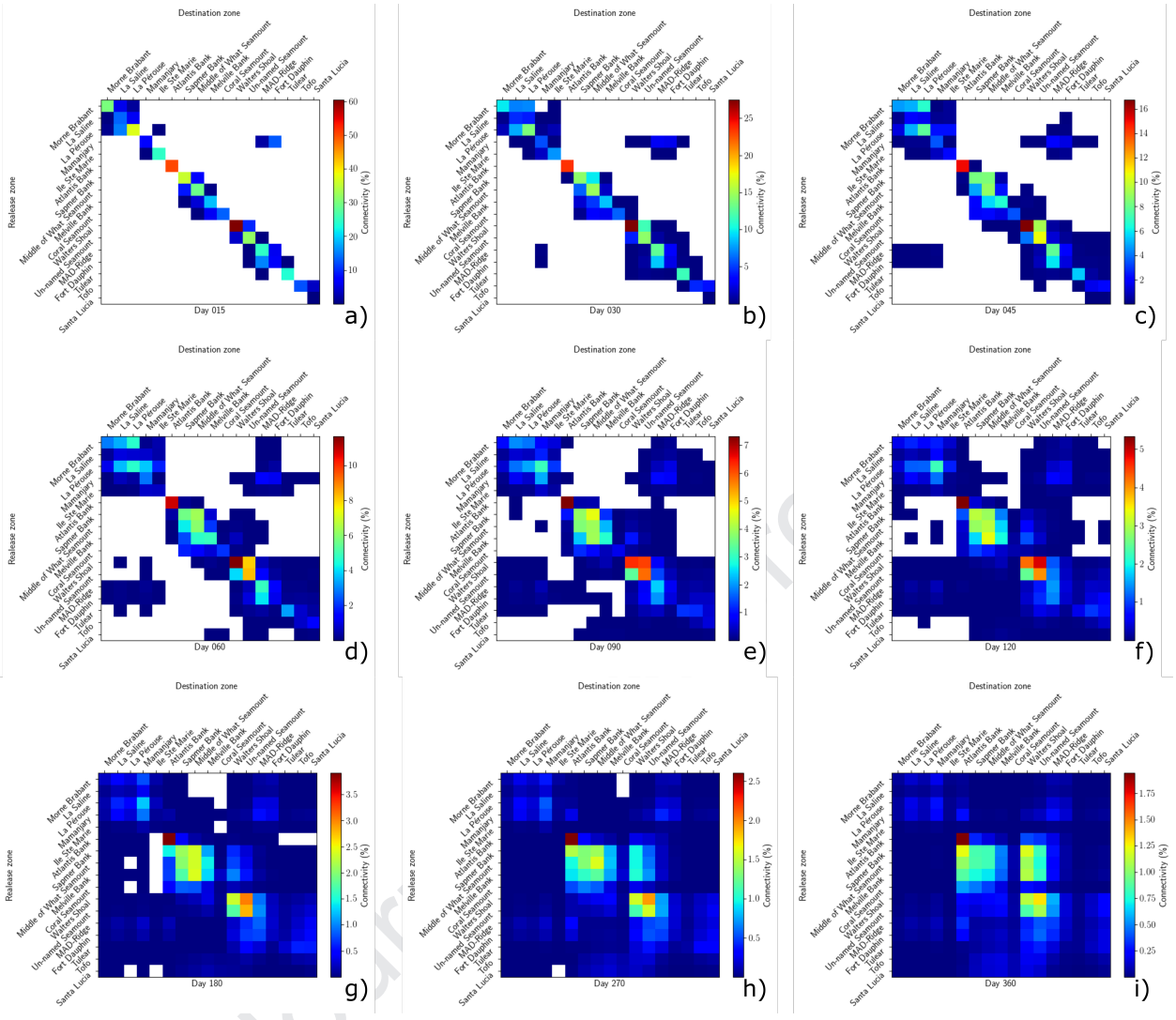
Destination zone
Realease zone
Connectivity (%)
Day 015
a)
Day 030
b)
Day 045
c)
Day 060
d)
Day 090
e)
Day 120
f)
Day 180
g)
Day 270
h)
Day 360
i)
Morne Brabant
La Saline
La Perouse
Mamanjay
Ile Ste Marie
Atlantis Bank
Sapmer Bank
Middle of What Seamount
Melville Bank
Coral Seamount
Walters Shoal
Un-named Seamount
MAD-Ridge
Fort Dauphin
Tolear
Tofo
Santa Lucia

Declaration of interests

☒ The authors declare that they have no known competing financial interests or personal relationships that could have appeared to influence the work reported in this paper.

☐The authors declare the following financial interests/personal relationships which may be considered as potential competing interests: